

NOVEL DEEP LEARNING MODELS AND TECHNIQUES FOR EFFECTIVE AND EFFICIENT HANDLING OF MULTIPLE DATA MODALITIES

Qiang Shawn Cheng

Institute for Biomedical Informatics

Department of Internal Medicine

Department of Computer Science

BRIEF OUTLINE

Four Topics

- A New Technique for Tabular Data Learning Problems
- A New Deep Learning Model for Long-Term Time Series Forecasting
- A New Diversity-Aware Tensor-Formulated Multi-View Clustering Technique
- A New Deep Learning Model for Time Series Classification
- (Optional) An Unsupervised Circadian Phase Inference Technique for Multi-Omics Data with Applications to Neurodegenerative Diseases

ACKNOWLEDGEMENT AND DISCLAIMER

The presented contents are based on joint work with Md Atik Ahamed, Aram Ansary Ogholbake, Dr. Peng, et al.

The research is partially supported by NSF under Grant IIS 2327113 and ITE 2433190, and the NIH under Grants R21AG070909, P30AG072946, and R01HD101508-01. I declare that the results presented in this talk do not pose any potential conflicts of interest with any funding agencies or collaborators involved in this research. The findings and conclusions are based on impartial and objective analysis, and no external influences have compromised the integrity of this work.

1ST TOPIC: A NEW DEEP LEARNING APPROACH FOR HANDLING TABULAR DATA

Motivation

- Importance of tabular data across domains
 - Structured format; mixed types; predominant in various domains
- Challenges with existing deep learning models for tabular data
 - Classical methods (MLP, XGBoost, LR): **accuracy**
 - Deep learning models (TabNet, CNN-based, DCN): **accuracy**
 - Transformer-based models (AutoInt, TabTransformer, FT-former, TransTab): **efficiency, accessibility, and scalability**
 - Self-Supervised Learning models (VIME, SCARF): **accuracy**
- Need for an accurate, efficient, scalable approach
 - Capturing correlations across features and samples
 - Also, existing models not suited to feature incremental learning

NEW MODEL: MAMBATAB

- Novel approach leveraging structured state-space model (SSM)

$$dh(t)/dt = A h(t) + B u(t), \quad x(t) = C h(t),$$

- Based on Mamba, an SSM variant

$$h_k = \bar{A} h_{k-1} + \bar{B} u_k, \quad x_k = C h_k, \quad \bar{A} = \exp(\Delta A), \quad \bar{B} = (\Delta A)^{-1}(\exp(\Delta A) - I)\Delta B.$$

- B, C, Δ : time varying (dependent on input); A: diagonal
- Advantages:
 - Small model size and number of parameters
 - Minimal preprocessing
 - High performance in accuracy
 - Linear complexity and linear scalability

MambaTab: A plug-and-play model for learning tabular data. MA Ahamed, Q Cheng, IEEE MIPR 2024.
Code available at GitHub.

METHOD - DATA PREPROCESSING

Simple, minimal preprocessing

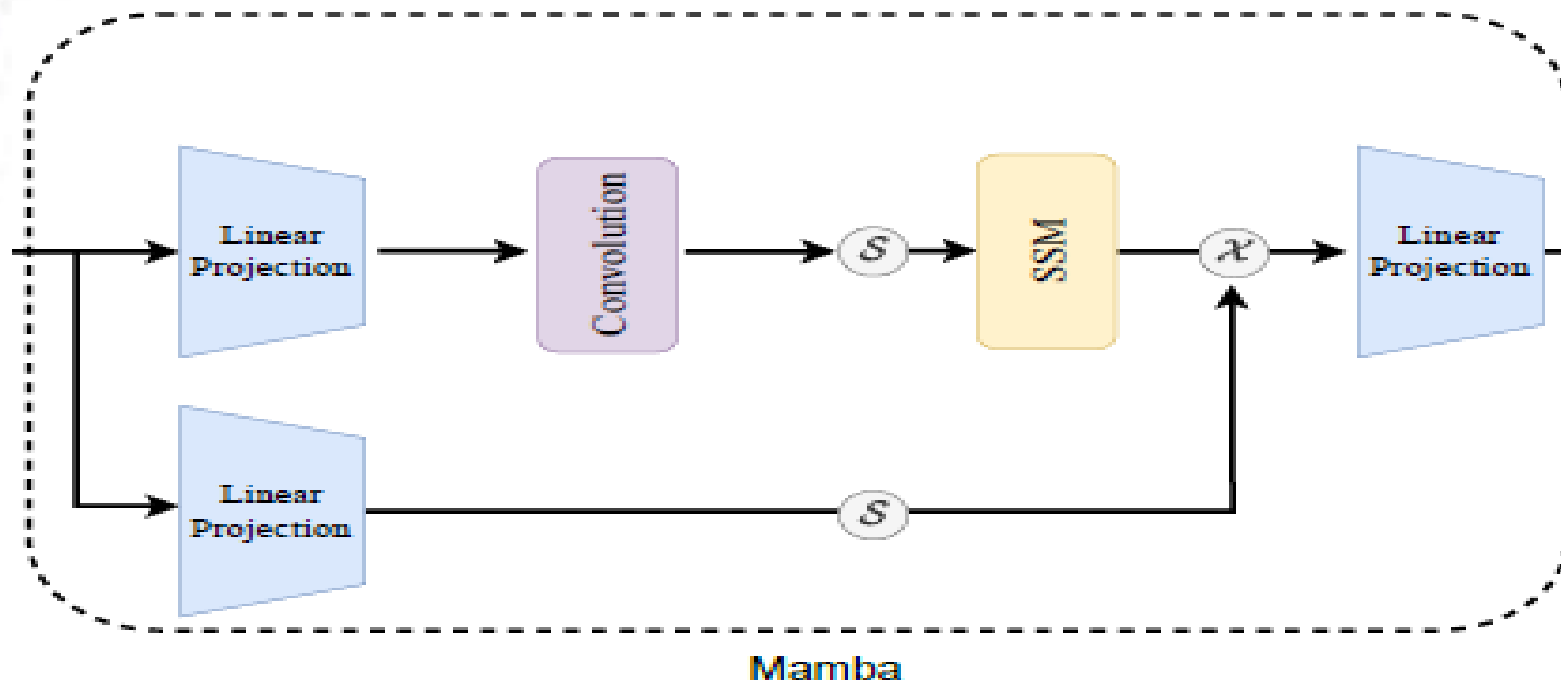
- Normalization and imputation
 - Min-max scaling

METHOD - EMBEDDING REPRESENTATION LEARNING

- Encoding categorical/Binary variables into numerical var. automatically
 - Each sample encoded into a token in a latent space
- Fully connected layer to learn embedded representations
- Enabling meaningful representations and incremental learning
- Layer normalization applied

METHOD - CASCADING MAMBA BLOCKS

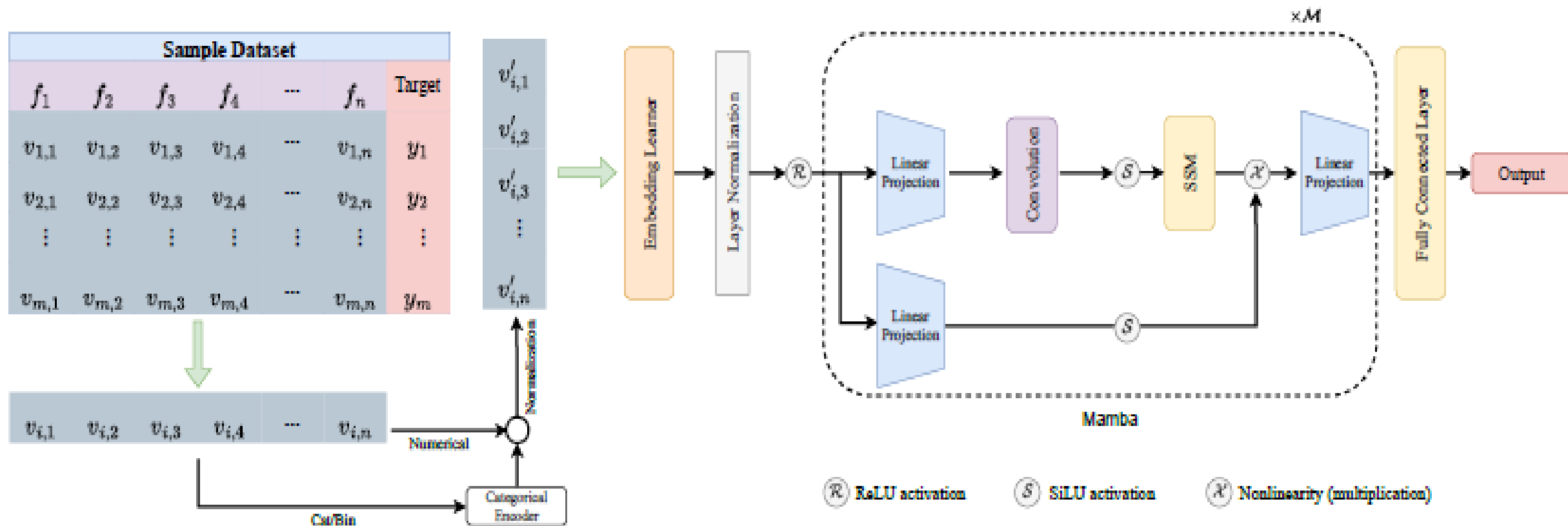
- Mamba block maps features into a feature space of the same dim.
- Utilizes linear projections, 1D causal convolution, SiLU activation, SSMs



- Context-dependent feature extraction and reasoning for long-range dependencies
- Cascading multiple Mamba blocks to seek important information w. various contexts

METHOD - OUTPUT PREDICTION

- Fully connected layer maps Mamba block outputs to predictions
- Sigmoid activation for probability scores



EXPERIMENTAL SETUP

- Datasets: 8 diverse public tabular datasets

| Dataset Name | Abbreviation | Datapoints | Train | Val | Test | Positive |
|-----------------|--------------|------------|-------|------|------|----------|
| Credit-g | CG | 1000 | 700 | 100 | 200 | 0.70 |
| Credit-approval | CA | 690 | 483 | 69 | 138 | 0.56 |
| Dresses-sales | DS | 500 | 350 | 50 | 100 | 0.42 |
| Adult | AD | 48842 | 34189 | 4884 | 9769 | 0.24 |
| Cylinder-bands | CB | 540 | 378 | 54 | 108 | 0.58 |
| Blastchar | BL | 7043 | 4930 | 704 | 1409 | 0.27 |
| Insurance-co | IO | 5822 | 4075 | 582 | 1165 | 0.06 |
| Income-1995 | IC | 32561 | 22792 | 3256 | 6513 | 0.24 |

- Baselines: 12 SOTA models - LR, XGBoost, MLP, SNN, TabNet, DCN, AutoInt, TabTransformer, FT-Transformer, VIME, SCARF, TransTab
- Settings: Vanilla supervised learning, feature incremental learning
- Metrics: AUROC

RESULTS - VANILLA SUPERVISED LEARNING

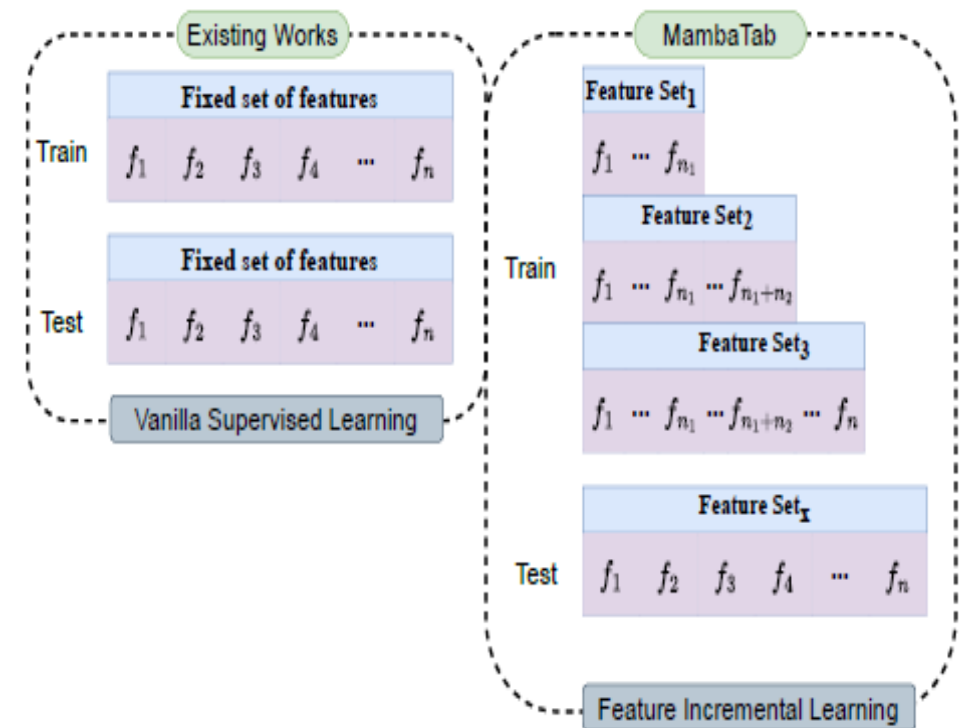
AUROC results on 8 datasets (averaged over 10 runs)

| Methods | Datasets | | | | | | | |
|------------|--------------|--------------|--------------|--------------|--------------|--------------|--------------|--------------|
| | CG | CA | DS | AD | CB | BL | IO | IC |
| LR | 0.720 | 0.836 | 0.557 | 0.851 | 0.748 | 0.801 | 0.769 | 0.860 |
| XGBoost | 0.726 | 0.895 | 0.587 | 0.912 | 0.892 | 0.821 | 0.758 | 0.925 |
| MLP | 0.643 | 0.832 | 0.568 | 0.904 | 0.613 | 0.832 | 0.779 | 0.893 |
| SNN | 0.641 | 0.880 | 0.540 | 0.902 | 0.621 | 0.834 | 0.794 | 0.892 |
| TabNet | 0.585 | 0.800 | 0.478 | 0.904 | 0.680 | 0.819 | 0.742 | 0.896 |
| DCN | 0.739 | 0.870 | 0.674 | 0.913 | 0.848 | 0.840 | 0.768 | 0.915 |
| AutoInt | 0.744 | 0.866 | 0.672 | 0.913 | 0.808 | 0.844 | 0.762 | 0.916 |
| TabTrans | 0.718 | 0.860 | 0.648 | 0.914 | 0.855 | 0.820 | 0.794 | 0.882 |
| FT-Trans | 0.739 | 0.859 | 0.657 | 0.913 | 0.862 | 0.841 | 0.793 | 0.915 |
| VIME | 0.735 | 0.852 | 0.485 | 0.912 | 0.769 | 0.837 | 0.786 | 0.908 |
| SCARF | 0.733 | 0.861 | 0.663 | 0.911 | 0.719 | 0.833 | 0.758 | 0.905 |
| TransTab | 0.768 | 0.881 | 0.643 | 0.907 | 0.851 | 0.845 | 0.822 | 0.919 |
| MambaTab-D | 0.771 | 0.954 | 0.643 | 0.906 | 0.862 | 0.852 | 0.785 | 0.906 |
| MambaTab-T | 0.801 | 0.963 | 0.681 | 0.914 | 0.896 | 0.854 | 0.812 | 0.920 |

- MambaTab outperforms baselines on majority datasets
- Hyperparameter tuning (MambaTab-T) improves upon default model

RESULTS - FEATURE INCREMENTAL LEARNING

AUROC results under feature incremental setting



| Methods | Datasets | | | | | | | |
|-------------------|--------------|--------------|--------------|--------------|--------------|--------------|--------------|--------------|
| | CG | CA | DS | AD | CB | BL | IO | IC |
| LR | 0.670 | 0.773 | 0.475 | 0.832 | 0.727 | 0.806 | 0.655 | 0.825 |
| XGBoost | 0.608 | 0.817 | 0.527 | 0.891 | 0.778 | 0.816 | 0.692 | 0.898 |
| MLP | 0.586 | 0.676 | 0.516 | 0.890 | 0.631 | 0.825 | 0.626 | 0.885 |
| SNN | 0.583 | 0.738 | 0.442 | 0.888 | 0.644 | 0.818 | 0.643 | 0.881 |
| TabNet | 0.573 | 0.689 | 0.419 | 0.886 | 0.571 | 0.837 | 0.680 | 0.882 |
| DCN | 0.674 | 0.835 | 0.578 | 0.893 | 0.778 | 0.840 | 0.660 | 0.891 |
| AutoInt | 0.671 | 0.825 | 0.563 | 0.893 | 0.769 | 0.836 | 0.676 | 0.887 |
| TabTrans | 0.653 | 0.732 | 0.584 | 0.856 | 0.784 | 0.792 | 0.674 | 0.828 |
| FT-Trans | 0.662 | 0.824 | 0.626 | 0.892 | 0.768 | 0.840 | 0.645 | 0.889 |
| VIME | 0.621 | 0.697 | 0.571 | 0.892 | 0.769 | 0.803 | 0.683 | 0.881 |
| SCARF | 0.651 | 0.753 | 0.556 | 0.891 | 0.703 | 0.829 | 0.680 | 0.887 |
| TransTab | 0.741 | 0.879 | 0.665 | 0.894 | 0.791 | 0.841 | 0.739 | 0.897 |
| MambaTab-D | 0.787 | 0.961 | 0.669 | 0.904 | 0.860 | 0.853 | 0.783 | 0.908 |

- MambaTab outperforms TransTab and other baselines with default hyperparameters on all datasets

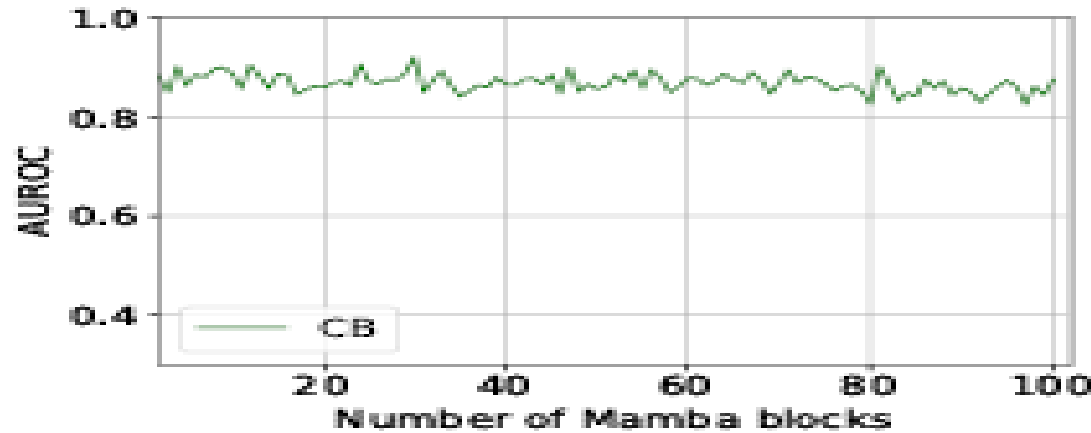
ANALYSIS - PARAMETER EFFICIENCY

Comparing learnable parameters of MambaTab vs Transformers

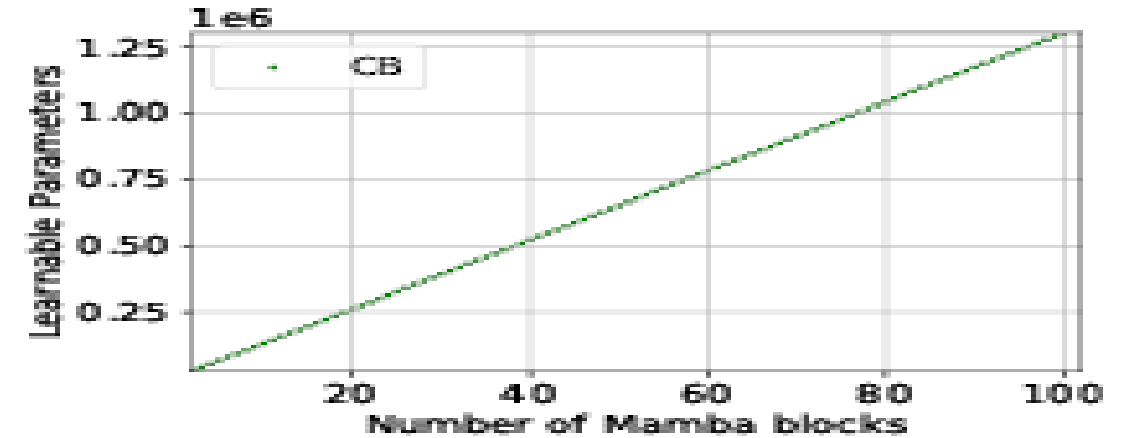
| Methods | Datasets | | | | | | | |
|------------|------------|------------|------------|-------------|------------|------------|------------|------------|
| | CG | CA | DS | AD | CB | BL | IO | IC |
| TabTrans | 2.7M | 1.2M | 2.0M | 1.2M | 6.5M | 3.4M | 87.0M | 1.0M |
| FT-Trans | 176K | 176K | 179K | 178K | 203K | 176K | 193K | 177K |
| TransTab | 4.2M | 4.2M | 4.2M | 4.2M | 4.2M | 4.2M | 4.2M | 4.2M |
| MambaTab-D | 13K | 13K | 13K | 13K | 14K | 13K | 15K | 13K |
| MambaTab-T | 50K | 38K | 5K | 255K | 30K | 11K | 13K | 10K |

- MambaTab uses <1% parameters of TransTab while achieving better performance

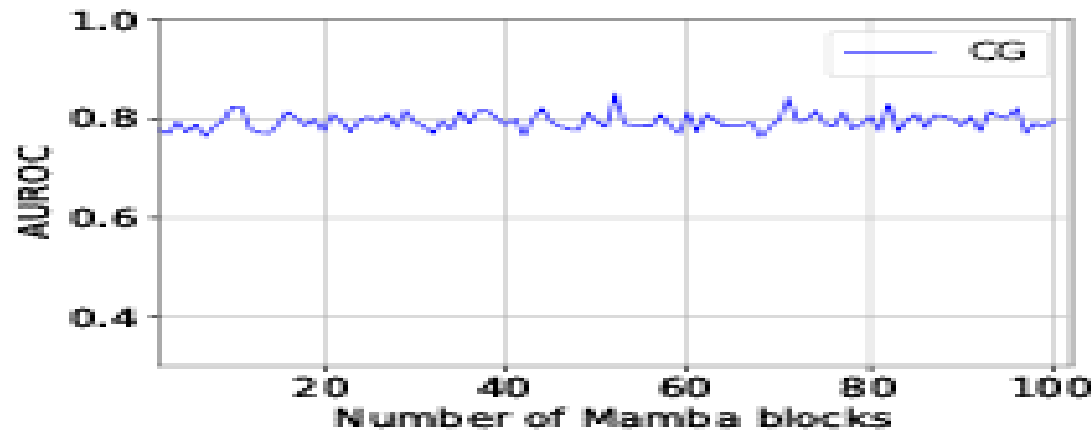
ANALYSIS - SCALABILITY AND ABLATION STUDY



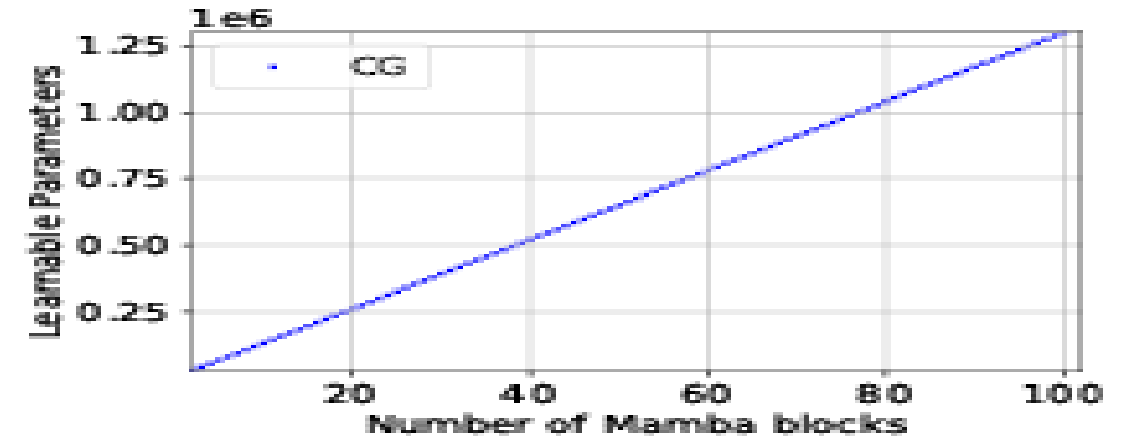
(a) AUROC results (CB)



(b) Learnable parameters (CB)



(c) AUROC results (CG)



(d) Learnable parameters (CG)

- Extensive hyper-parameter sensitivity study and structural ablations study
 - More in the paper – MambaTab - Not shown here

BRIEF CONCLUSION OF THE 1ST TOPIC

- MambaTab: out-of-the-box, plug-and-play model for tabular data
- Simple architecture, minimal preprocessing, superior performance, parameter-efficient
- We also obtained superior results for SSL, not shown here
- Holds promise for enabling wider practical applications across domains

2ND TOPIC – A DEEP LEARNING MODEL FOR TIME SERIES LONG-TERM FORECASTING

- Importance of long-term time-series forecasting (LTSF) across domains
- Challenges in LTSF
 - capturing long-term dependencies
 - scalability
 - computational efficiency
- Limitations of existing approaches
 - Non-Transformer-based: Classical models (ARIMA, RNN, GARCH), Linear models – MLP (DLinear, RLinear, TiDE), CNN (TimesNet, Scinet)
linear complexity and scalability, may not capture LT dependency, accuracy
 - Transformer-based SL models (iTransformer, PatchTST, CrossFormer): can capture LT dependency, SOTA accuracy, quadratic complexity and not scalable well
 - SSL Representation Learning: typically Transformer-based (TST, TS-TCC):
not as competitive as SL models in accuracy

NEW MODEL: TIMEMACHINE

- Novel approach leveraging structured state-space models (SSMs), Mamba
- Exploiting unique properties of time series data to produce salient contextual cues at multi-scales
- Innovative integrated quadruple-Mamba architecture
- Key Innovations
 - First to leverage purely SSM modules for context-aware LTSF with linear scalability and small memory footprints
 - Unifies handling of channel-mixing and channel-independence situations
 - Selects contents for prediction incorporating global and local contexts at different scales

METHOD - DATA PREPROCESSING AND EMBEDDED REPRESENTATIONS

Preprocessing

- Normalization options: RevIN or Z-score
- Channel mixing vs. channel independence handling

Embedded Representation

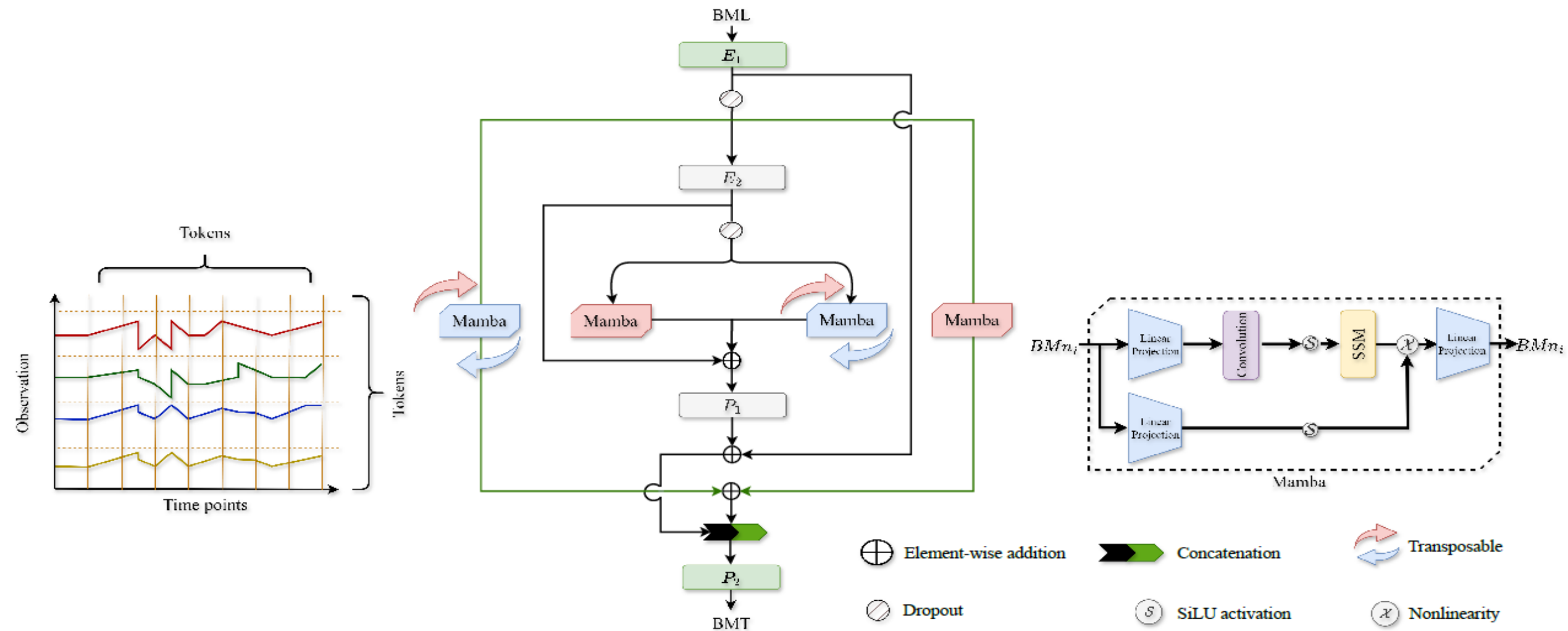
- Two-stage embedded representations using MLPs
- Enables handling variable input sequence lengths

METHOD - INTEGRATED QUADRUPLE MAMBAS

- Two pairs of Mambas at 2 embedding levels
- Capture long-term dependencies and provide local contexts
- Handling channel-mixing and channel-independence cases
- Transposable Mambas for unified architecture

METHOD - OUTPUT PROJECTION AND ARCHITECTURE

- Two-stage output projection using MLPs
- Residual connections for stabilization and overfitting reduction



EXPERIMENTAL SETUP

- Datasets: 7 standard benchmark datasets

| Dataset (\mathcal{D}) | Channels (M) | Time Points | Frequency |
|---------------------------|--------------|-------------|------------|
| Weather | 21 | 52696 | 10 Minutes |
| Traffic | 862 | 17544 | Hourly |
| Electricity | 321 | 26304 | Hourly |
| ETTh1 | 7 | 17420 | Hourly |
| ETTh2 | 7 | 17420 | Hourly |
| ETTm1 | 7 | 69680 | 15 Minutes |
| ETTm2 | 7 | 69680 | 15 Minutes |

- Baselines: 11 SOTA models
- Metrics: MSE and MAE

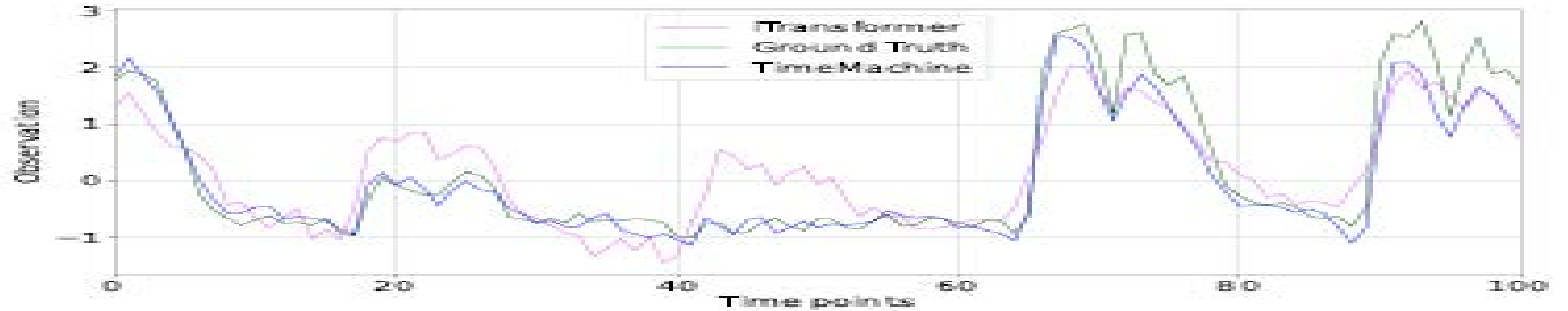
RESULTS - QUANTITATIVE

| Methods→ | | TimeMachine | | iTransformer | | RLinear | | PatchTST | | Crossformer | | TiDE | | TimesNet | | DLinear | | SCINet | | FEDformer | | Stationary | | Autoformer | |
|---------------|-----|--------------|--------------|--------------|--------------|---------|-------|--------------|-------|--------------|-------|-------|-------|----------|-------|---------|-------|--------|-------|--------------|-------|------------|-------|------------|-------|
| \mathcal{D} | T | MSE | MAE | MSE | MAE | MSE | MAE | MSE | MAE | MSE | MAE | MSE | MAE | MSE | MAE | MSE | MAE | MSE | MAE | MSE | MAE | MSE | MAE | MSE | MAE |
| Weather | 96 | 0.164 | 0.208 | 0.174 | 0.214 | 0.192 | 0.232 | 0.177 | 0.218 | 0.158 | 0.230 | 0.202 | 0.261 | 0.172 | 0.220 | 0.196 | 0.255 | 0.221 | 0.306 | 0.217 | 0.296 | 0.173 | 0.223 | 0.266 | 0.336 |
| | 192 | 0.211 | 0.250 | 0.221 | 0.254 | 0.240 | 0.271 | 0.225 | 0.259 | 0.206 | 0.277 | 0.242 | 0.298 | 0.219 | 0.261 | 0.237 | 0.296 | 0.261 | 0.340 | 0.276 | 0.336 | 0.245 | 0.285 | 0.307 | 0.367 |
| | 336 | 0.256 | 0.290 | 0.278 | 0.296 | 0.292 | 0.307 | 0.278 | 0.297 | 0.272 | 0.335 | 0.287 | 0.335 | 0.280 | 0.306 | 0.283 | 0.335 | 0.309 | 0.378 | 0.339 | 0.380 | 0.321 | 0.338 | 0.359 | 0.395 |
| | 720 | 0.342 | 0.343 | 0.358 | 0.349 | 0.364 | 0.353 | 0.354 | 0.348 | 0.398 | 0.418 | 0.351 | 0.386 | 0.365 | 0.359 | 0.345 | 0.381 | 0.377 | 0.427 | 0.403 | 0.428 | 0.414 | 0.410 | 0.419 | 0.428 |
| Traffic | 96 | 0.397 | 0.268 | 0.395 | 0.268 | 0.649 | 0.389 | 0.544 | 0.359 | 0.522 | 0.290 | 0.805 | 0.493 | 0.593 | 0.321 | 0.650 | 0.396 | 0.788 | 0.499 | 0.587 | 0.366 | 0.612 | 0.338 | 0.613 | 0.388 |
| | 192 | 0.417 | 0.274 | 0.417 | 0.276 | 0.601 | 0.366 | 0.540 | 0.354 | 0.530 | 0.293 | 0.756 | 0.474 | 0.617 | 0.336 | 0.598 | 0.370 | 0.789 | 0.505 | 0.604 | 0.373 | 0.613 | 0.340 | 0.616 | 0.382 |
| | 336 | 0.433 | 0.281 | 0.433 | 0.283 | 0.609 | 0.369 | 0.551 | 0.358 | 0.558 | 0.305 | 0.762 | 0.477 | 0.629 | 0.336 | 0.605 | 0.373 | 0.797 | 0.508 | 0.621 | 0.383 | 0.618 | 0.328 | 0.622 | 0.337 |
| | 720 | 0.467 | 0.300 | 0.467 | 0.302 | 0.647 | 0.387 | 0.586 | 0.375 | 0.589 | 0.328 | 0.719 | 0.449 | 0.640 | 0.350 | 0.645 | 0.394 | 0.841 | 0.523 | 0.626 | 0.382 | 0.653 | 0.355 | 0.660 | 0.408 |
| Electricity | 96 | 0.142 | 0.236 | 0.148 | 0.240 | 0.201 | 0.281 | 0.195 | 0.285 | 0.219 | 0.314 | 0.237 | 0.329 | 0.168 | 0.272 | 0.197 | 0.282 | 0.247 | 0.345 | 0.193 | 0.308 | 0.169 | 0.273 | 0.201 | 0.317 |
| | 192 | 0.158 | 0.250 | 0.162 | 0.253 | 0.201 | 0.283 | 0.199 | 0.289 | 0.231 | 0.322 | 0.236 | 0.330 | 0.184 | 0.289 | 0.196 | 0.285 | 0.257 | 0.355 | 0.201 | 0.315 | 0.182 | 0.286 | 0.222 | 0.334 |
| | 336 | 0.172 | 0.268 | 0.178 | 0.269 | 0.215 | 0.298 | 0.215 | 0.305 | 0.246 | 0.337 | 0.249 | 0.344 | 0.198 | 0.300 | 0.209 | 0.301 | 0.269 | 0.369 | 0.214 | 0.329 | 0.200 | 0.304 | 0.231 | 0.338 |
| | 720 | 0.207 | 0.298 | 0.225 | 0.317 | 0.257 | 0.331 | 0.256 | 0.337 | 0.280 | 0.363 | 0.284 | 0.373 | 0.220 | 0.320 | 0.245 | 0.333 | 0.299 | 0.390 | 0.246 | 0.355 | 0.222 | 0.321 | 0.254 | 0.361 |
| ETTh1 | 96 | 0.364 | 0.387 | 0.386 | 0.405 | 0.386 | 0.395 | 0.414 | 0.419 | 0.423 | 0.448 | 0.479 | 0.464 | 0.384 | 0.402 | 0.386 | 0.400 | 0.654 | 0.599 | 0.376 | 0.419 | 0.513 | 0.491 | 0.449 | 0.459 |
| | 192 | 0.415 | 0.416 | 0.441 | 0.436 | 0.437 | 0.424 | 0.460 | 0.445 | 0.471 | 0.474 | 0.525 | 0.492 | 0.436 | 0.429 | 0.437 | 0.432 | 0.719 | 0.631 | 0.420 | 0.448 | 0.534 | 0.504 | 0.500 | 0.482 |
| | 336 | 0.429 | 0.421 | 0.487 | 0.458 | 0.479 | 0.446 | 0.501 | 0.466 | 0.570 | 0.546 | 0.565 | 0.515 | 0.491 | 0.469 | 0.481 | 0.459 | 0.778 | 0.659 | 0.459 | 0.465 | 0.588 | 0.535 | 0.521 | 0.496 |
| | 720 | 0.458 | 0.453 | 0.503 | 0.491 | 0.481 | 0.470 | 0.500 | 0.488 | 0.653 | 0.621 | 0.594 | 0.558 | 0.521 | 0.500 | 0.519 | 0.516 | 0.836 | 0.699 | 0.506 | 0.507 | 0.643 | 0.616 | 0.514 | 0.512 |
| ETTh2 | 96 | 0.275 | 0.334 | 0.297 | 0.349 | 0.288 | 0.338 | 0.302 | 0.348 | 0.745 | 0.584 | 0.400 | 0.440 | 0.340 | 0.374 | 0.333 | 0.387 | 0.707 | 0.621 | 0.358 | 0.397 | 0.476 | 0.458 | 0.346 | 0.388 |
| | 192 | 0.349 | 0.381 | 0.380 | 0.400 | 0.374 | 0.390 | 0.388 | 0.400 | 0.877 | 0.656 | 0.528 | 0.509 | 0.402 | 0.414 | 0.477 | 0.476 | 0.860 | 0.689 | 0.429 | 0.439 | 0.512 | 0.493 | 0.456 | 0.452 |
| | 336 | 0.340 | 0.381 | 0.428 | 0.432 | 0.415 | 0.426 | 0.426 | 0.433 | 1.043 | 0.731 | 0.643 | 0.571 | 0.452 | 0.452 | 0.594 | 0.541 | 1.000 | 0.744 | 0.496 | 0.487 | 0.552 | 0.551 | 0.482 | 0.486 |
| | 720 | 0.411 | 0.433 | 0.427 | 0.445 | 0.420 | 0.440 | 0.431 | 0.446 | 1.104 | 0.763 | 0.874 | 0.679 | 0.462 | 0.468 | 0.831 | 0.657 | 1.249 | 0.838 | 0.463 | 0.474 | 0.562 | 0.560 | 0.515 | 0.511 |
| ETTm1 | 96 | 0.317 | 0.355 | 0.334 | 0.368 | 0.355 | 0.376 | 0.329 | 0.367 | 0.404 | 0.426 | 0.364 | 0.387 | 0.338 | 0.375 | 0.345 | 0.372 | 0.418 | 0.438 | 0.379 | 0.419 | 0.386 | 0.398 | 0.505 | 0.475 |
| | 192 | 0.357 | 0.378 | 0.377 | 0.391 | 0.391 | 0.392 | 0.367 | 0.385 | 0.450 | 0.451 | 0.398 | 0.404 | 0.374 | 0.387 | 0.380 | 0.389 | 0.439 | 0.450 | 0.426 | 0.441 | 0.459 | 0.444 | 0.553 | 0.496 |
| | 336 | 0.379 | 0.399 | 0.426 | 0.420 | 0.424 | 0.415 | 0.399 | 0.410 | 0.532 | 0.515 | 0.428 | 0.425 | 0.410 | 0.411 | 0.413 | 0.413 | 0.490 | 0.485 | 0.445 | 0.459 | 0.495 | 0.464 | 0.621 | 0.537 |
| | 720 | 0.445 | 0.436 | 0.491 | 0.459 | 0.487 | 0.450 | 0.454 | 0.439 | 0.666 | 0.589 | 0.487 | 0.461 | 0.478 | 0.450 | 0.474 | 0.453 | 0.595 | 0.550 | 0.543 | 0.490 | 0.585 | 0.516 | 0.671 | 0.561 |
| ETTm2 | 96 | 0.175 | 0.256 | 0.180 | 0.264 | 0.182 | 0.265 | 0.175 | 0.259 | 0.287 | 0.366 | 0.207 | 0.305 | 0.187 | 0.267 | 0.193 | 0.292 | 0.286 | 0.377 | 0.203 | 0.287 | 0.192 | 0.274 | 0.255 | 0.339 |
| | 192 | 0.239 | 0.299 | 0.250 | 0.309 | 0.246 | 0.304 | 0.241 | 0.302 | 0.414 | 0.492 | 0.290 | 0.364 | 0.249 | 0.309 | 0.284 | 0.362 | 0.399 | 0.445 | 0.269 | 0.328 | 0.280 | 0.339 | 0.281 | 0.340 |
| | 336 | 0.287 | 0.332 | 0.311 | 0.348 | 0.307 | 0.342 | 0.305 | 0.343 | 0.597 | 0.542 | 0.377 | 0.422 | 0.321 | 0.351 | 0.369 | 0.427 | 0.637 | 0.591 | 0.325 | 0.366 | 0.334 | 0.361 | 0.339 | 0.372 |
| | 720 | 0.371 | 0.385 | 0.412 | 0.407 | 0.407 | 0.398 | 0.402 | 0.400 | 1.730 | 1.042 | 0.558 | 0.524 | 0.408 | 0.403 | 0.554 | 0.522 | 0.960 | 0.735 | 0.421 | 0.415 | 0.417 | 0.413 | 0.433 | 0.432 |

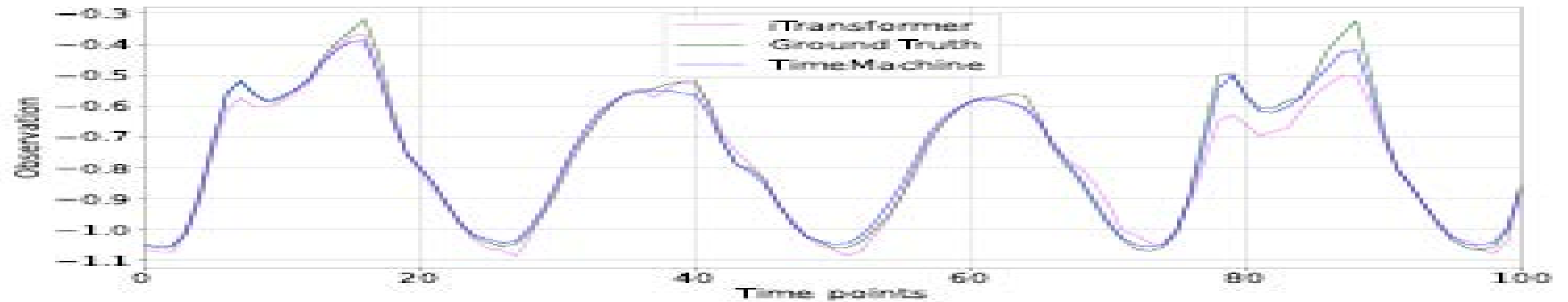
- Superior performance in almost all cases
- Effectiveness in handling varying number of channels and look-back windows

RESULTS - QUALITATIVE

Visually comparing TimeMachine with best-performing baselines



(a) Electricity

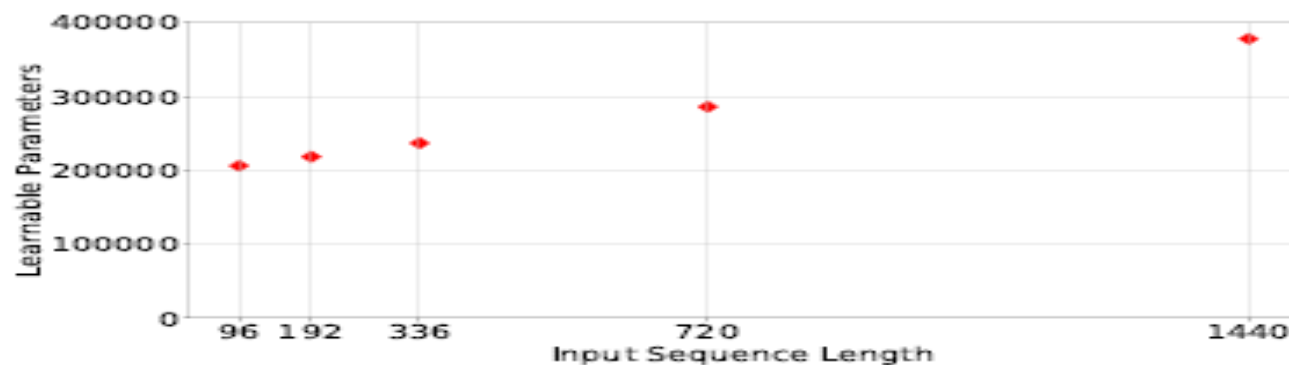


(b) Traffic

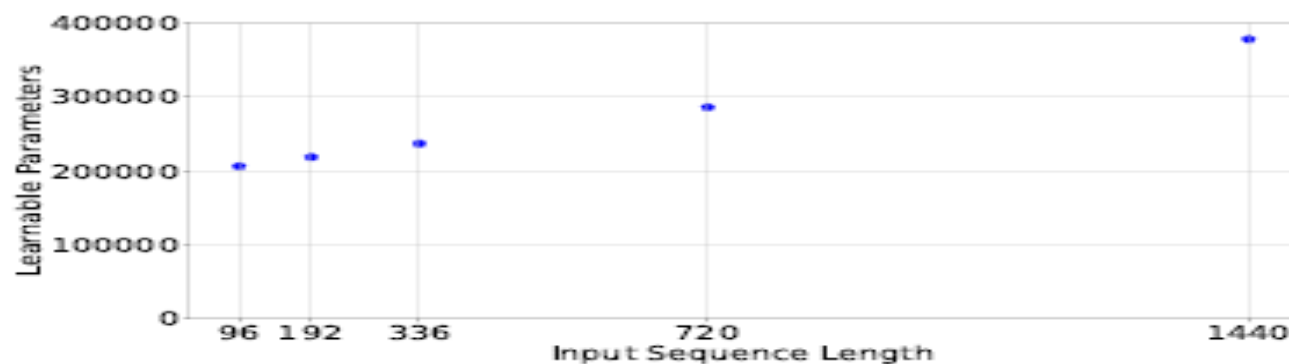
- TimeMachine aligns well with ground truth

ANALYSIS - MEMORY FOOTPRINT AND SCALABILITY

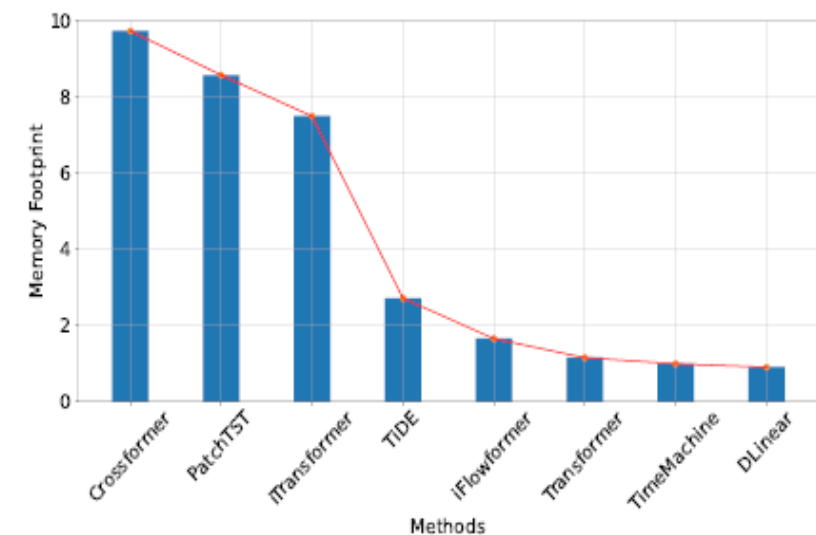
- Comparison of memory footprints with baselines (Traffic: 862 channels; Weather: 21 channels)
- Linear scalability in terms of learnable parameters



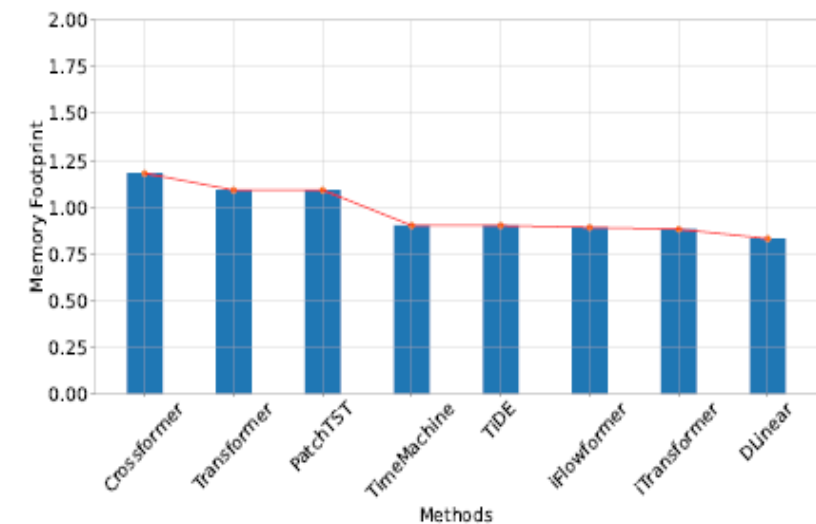
(a) ETTh2



(b) Weather



(a) Traffic



(b) Weather

BRIEF CONCLUSION OF TOPIC 2

- TimeMachine: novel deep learning model for LTSF
- Superior performance, linear scalability, small memory footprints
- Potential for future exploration in self-supervised learning setting

TOPIC 3 - CROSS-VIEW DIVERSITY EMBEDDED CONSENSUS LEARNING FOR MULTI-VIEW CLUSTERING

- Importance of multi-view clustering (MVC)
 - Clustering is fundamental;
 - Data from multiple sources often need multi-view clustering
- Challenges in MVC
 - How to find **consensus information** from multiple views
 - Diversity not properly embedded – **redundant information across views** often emphasized
 - How to simultaneously learn consensus and diversity information
- Limitations of existing methods
 - Existing methods follow 2 steps: affinity matrix; spectral clustering
 - for affinity matrix, low-rank tensor recovery: tensor nuclear norm
 - Diversity is not incorporated
 - High-order neighbor information is rarely considered

RELATED WORK

Two main categories of MVC methods

- Spectral clustering (SPC)-based subspace clustering: Markov random walk
 - RMSC: transition prob. matrix for each view, common low-rank stochastic matrix by combining w. Markov mixture
 - MVC: low-rank tensor recovery from tensor nuclear norm
 - ETLMSC: essential low-rank tensor
- Graph-based subspace clustering: affinity matrix from similarity matrix
 - Focus on graph-based methods using similarity matrix

ETLMSC:

- Multi-view data: $\{\mathbf{X}^{(v)}\}_{v=1}^V$ where $\mathbf{X}^{(v)} \in \mathbb{R}^{d_v \times n}$
- Trans. Prob. Matrix-based tensor: $\mathcal{P} \in \mathbb{R}^{n \times n \times V}$

$$\min_{\mathbf{Z}, \mathcal{E} \in \mathbb{R}^{n \times n \times V}} \|\mathbf{Z}\|_{\otimes} + \lambda \|\mathcal{E}\|_{2,1} \quad s.t. \quad \mathcal{P} = \mathbf{Z} + \mathcal{E},$$

KEY INNOVATIONS

- Recovering low-rank essential tensor from cross-order neighbor graph tensor
- Embedding auto-adjusted weighting vector for cross-view diversity and consensus
- Efficient optimization algorithm with convergence guarantee
- Superior performance over baselines

NEW METHOD: CCL-MVC

- Constructing cross-order neighbor tensor
 - Higher-order neighbor relationships
 - Fine-grained probability tensor with local structure preservation

$$\mathcal{P}_K^{(v)} = \sum_{k=1}^K \frac{(\mathcal{P}^{(v)})^k + ((\mathcal{P}^{(v)})^k)^T}{2}$$

- Recovering low-rank essential tensor: log-based rank and sparsity approx.

$$\min_{\mathcal{Z}, \mathcal{E}} \|\mathcal{Z}\|_{\textcircled{R}} + \lambda \|\mathcal{E}\|_{\textcircled{S}} \quad s.t. \quad \mathcal{P}_K = \mathcal{Z} + \mathcal{E}$$

$$\|\mathcal{Z}\|_{\textcircled{R}} = \sum_{v=1}^V \sum_{i=1}^n \log(1 + \sigma_i(\hat{\mathcal{Z}}^{(v)}))$$

$$\|\mathcal{E}\|_{\textcircled{S}} = \sum_{j=1}^n \log(1 + (\sum_{i=1}^n \sum_{v=1}^V \mathcal{E}_{ijv}^2)^{1/2})$$

- C Peng, Y Liu, K Kang, Y Chen, X Wu, A Cheng, Z Kang, C Chen, and Q Cheng. Hyperspectral image denoising using nonconvex local low-rank and sparse separation with spatial-spectral total variation regularization. IEEE Transactions on Geoscience and Remote Sensing, 60:1–17, 2022.

C Peng, Z Kang, H Li, and Q Cheng. Subspace clustering using log-determinant rank approximation. ACM KDD, pp. 925–934, 2015

NEW METHOD: CCL-MVC

- Constructing consensus representation matrix

$$\min_{\mathcal{Z}, \mathcal{E}, w} \|\mathcal{Z}\|_{\textcircled{R}} + \lambda \|\mathcal{E}\|_{\textcircled{S}} + \alpha \sum_v \|Z_0 - w_v \mathcal{Z}^{(v)}\|_F^2$$
$$s.t. \mathcal{P}_K = \mathcal{Z} + \mathcal{E}, w_v \geq 0, \sum_v w_v = 1,$$

Z_0 : consensus affinity matrix fusing cross-view neighbor graphs

w_v : auto adjusted weights for the v -th view

- Twin learning for similarity and clustering: A unified kernel approach. Z Kang, C Peng, Q Cheng, AAAI, 2017.
- Kernel-driven similarity learning. Z Kang, C Peng, Q Cheng, Neurocomputing. 2017; 210-219.

CCL-MVC FORMULATION

- Incorporating Diversity Representation Matrix Learning
 - Auto-adjusted weighting vector for cross-view diversity
 - Embedding fusion into the model

$$\min_{\mathcal{P}_K = \mathcal{Z} + \mathcal{E}, w \geq 0, \sum_i w_i = 1} \|\mathcal{Z}\|_{\textcircled{\mathbb{R}}} + \lambda \|\mathcal{E}\|_{\textcircled{\mathbb{S}}} \\ + \alpha \sum_{v=1}^V \|\mathcal{Z}_0 - w_v \mathcal{Z}^{(v)}\|_F^2 + \beta \sum_{i,j=1}^V w_i w_j \text{Tr}((\mathcal{Z}^{(i)})^T \mathcal{Z}^{(j)}),$$

Cross-View Diversity Embedded Consensus Learning for Multi-View Clustering.
C Peng, K Zhang, Y Chen, C Chen, Q Cheng. IJCAI 2024.

OPTIMIZATION ALGORITHM

Alternating optimization with ALM

Sub-problems and solutions for each variable

- Optimization of \mathcal{Z} :
$$\min_{\mathcal{Z}} \alpha \sum_v \|Z_0 - w_v \mathcal{Z}^{(v)}\|_F^2 + \beta \sum_{i,j} w_i w_j \text{Tr}((\mathcal{Z}^{(i)})^T \mathcal{Z}^{(j)})$$
$$+ \frac{\rho}{2} \|\mathcal{Q} - \mathcal{Z} + \mathcal{Y}_1 / \rho\|_F^2 + \frac{\rho}{2} \|\mathcal{P}_K - \mathcal{Z} - \mathcal{E} + \mathcal{Y}_2 / \rho\|_F^2.$$
- Optimization of \mathcal{Q} :
$$\min_{\mathcal{Q}} \|\mathcal{Q}\|_{\mathbb{R}} + \frac{\rho}{2} \|\mathcal{Q} - \mathcal{Z} + \mathcal{Y}_1 / \rho\|_F^2.$$
- Optimization of \mathcal{E} :
$$\min_{\mathcal{E}} \lambda \|\mathcal{E}\|_{\mathbb{S}} + \frac{\rho}{2} \|\mathcal{P}_K - \mathcal{Z} - \mathcal{E} + \mathcal{Y}_2 / \rho\|_F^2$$
- Optimization of Z_0 , w: straightforward $\alpha \sum_v \|Z_0 - w_v \mathcal{Z}^{(v)}\|_F^2$
- Updating of \mathcal{Y}_1 , \mathcal{Y}_2 , and ρ : standard steps

CONVERGENCE ANALYSIS

Theorem 1: Boundedness of variable sequences

Theorem 1. Let t in the superscript denote the iteration number. Under assumptions that $\sum \frac{1}{\rho^t} < \infty$ and $\sum \frac{\rho^{t+1}}{(\rho^t)^2} < \infty$, and given a bounded initialization of the variables, the variable sequences $\{\mathcal{Z}^t\}$, $\{\mathcal{E}^t\}$, $\{\mathcal{Q}^t\}$, $\{Z_0^t\}$, $\{w^t\}$, $\{\mathcal{Y}_1^t\}$, and $\{\mathcal{Y}_2^t\}$ generated by our optimization algorithm are bounded.

Theorem 2: Convergence to a stationary point

Theorem 2. Let $\{\mathcal{Z}^t, \mathcal{E}^t, \mathcal{Q}^t, Z_0^t, w^t, \mathcal{Y}_1^t, \mathcal{Y}_2^t\}$ be a sequence generated by our algorithm. Under assumptions that $\sum \frac{1}{\rho^t} < \infty$, $\sum \frac{\rho^{t+1}}{(\rho^t)^2} < \infty$, $\rho^t(\mathcal{Q}^{t+1} - \mathcal{Q}^t) \rightarrow 0$, and $\rho^t(\mathcal{E}^{t+1} - \mathcal{E}^t) \rightarrow 0$, the sequence $\{\mathcal{Z}^t, \mathcal{E}^t, \mathcal{Q}^t, Z_0^t, w^t, \mathcal{Y}_1^t, \mathcal{Y}_2^t\}$ has at least one accumulation point. For any accumulation point, denoted as $\{\mathcal{Z}^*, \mathcal{E}^*, \mathcal{Q}^*, Z_0^*, w^*, \mathcal{Y}_1^*, \mathcal{Y}_2^*\}$, $\{\mathcal{Z}^*, \mathcal{E}^*, \mathcal{Q}^*, Z_0^*, w^*\}$ is a stationary point of the optimization problem in Eq. (5).

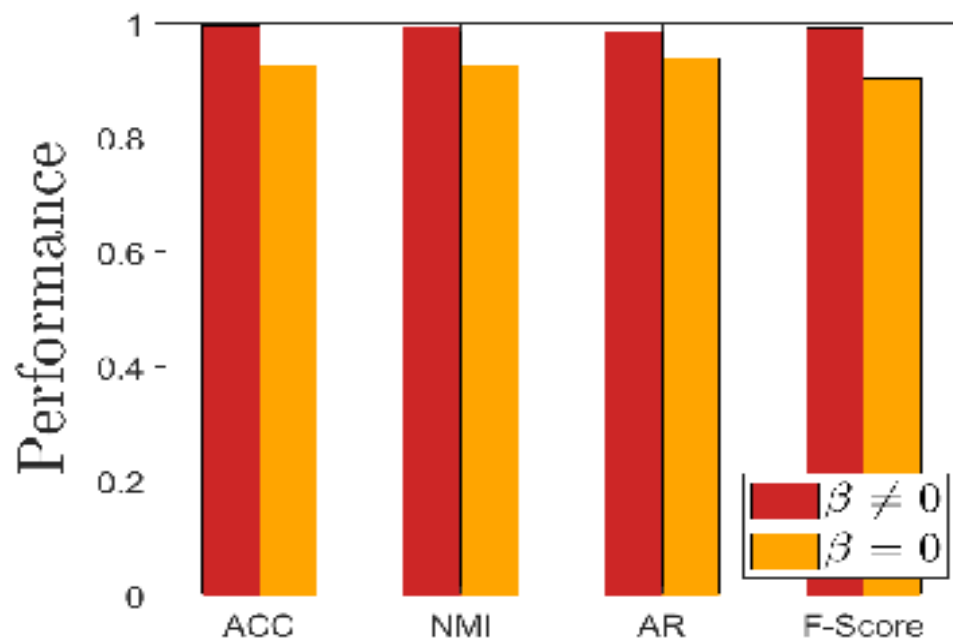
EXPERIMENTAL SETUP

- Datasets: 6 standard benchmark datasets
 - BBC-4view, BBC-Sport, Flowers, UCI-3view, StillDB, MITindoor,
- Evaluation metrics: 4 metrics
 - clustering accuracy (ACC), normalized mutual information (NMI), adjusted rand index (AR), F-Score
- Parameter settings
- Comparing our method with 17 SOTA baselines
 - CCL-MVC: Cross-view diversity embedded Consensus Learning for Multi-View Clustering
 - Superiority and stability

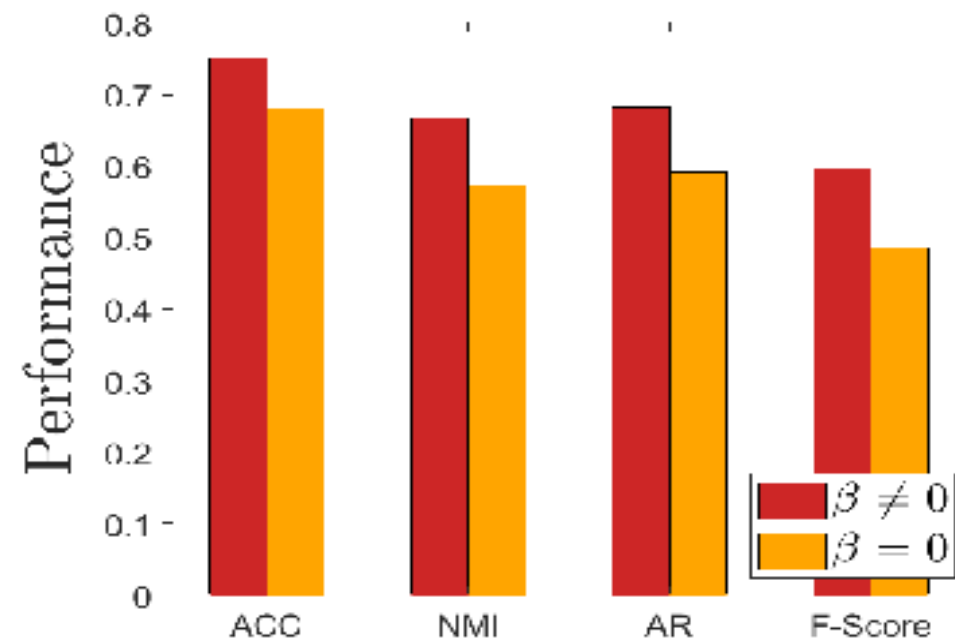
| Datasets | BBC-4view | | | | BBC-Sport | | | | Flowers | | | |
|---------------------|-------------|-------------|-------------|-------------|-------------|-------------|-------------|-------------|-------------|-------------|-------------|-------------|
| Methods | ACC | NMI | AR | F-Score | ACC | NMI | AR | F-Score | ACC | NMI | AR | F-Score |
| AWP | 0.904±0.000 | 0.760±0.000 | 0.797±0.000 | 0.845±0.000 | 0.809±0.000 | 0.723±0.000 | 0.726±0.000 | 0.796±0.000 | 0.435±0.000 | 0.430±0.000 | 0.246±0.000 | 0.292±0.000 |
| MvDSCN | 0.495±0.019 | 0.247±0.022 | 0.224±0.023 | 0.437±0.015 | 0.931±0.001 | 0.935±0.000 | 0.909±0.001 | 0.860±0.000 | 0.276±0.012 | 0.285±0.012 | 0.108±0.010 | 0.182±0.008 |
| OMVFC-LICAG | 0.718±0.000 | 0.586±0.000 | 0.584±0.000 | 0.688±0.000 | 0.724±0.000 | 0.571±0.000 | 0.397±0.000 | 0.627±0.000 | 0.397±0.000 | 0.404±0.000 | 0.208±0.000 | 0.259±0.000 |
| MLAN | 0.853±0.007 | 0.698±0.010 | 0.716±0.005 | 0.783±0.004 | 0.721±0.000 | 0.779±0.000 | 0.591±0.000 | 0.714±0.000 | 0.501±0.008 | 0.532±0.003 | 0.331±0.010 | 0.373±0.009 |
| GMC | 0.693±0.000 | 0.563±0.000 | 0.479±0.000 | 0.633±0.000 | 0.807±0.000 | 0.760±0.000 | 0.722±0.000 | 0.794±0.000 | 0.177±0.000 | 0.247±0.000 | 0.020±0.000 | 0.125±0.000 |
| UOMvSC | 0.391±0.000 | 0.170±0.000 | 0.105±0.000 | 0.267±0.000 | 0.529±0.000 | 0.302±0.000 | 0.209±0.000 | 0.415±0.000 | 0.507±0.000 | 0.508±0.000 | 0.313±0.000 | 0.355±0.000 |
| EOMSC-CA | 0.425±0.000 | 0.090±0.000 | 0.090±0.000 | 0.365±0.000 | 0.384±0.000 | 0.083±0.000 | 0.058±0.000 | 0.375±0.000 | 0.374±0.000 | 0.418±0.000 | 0.221±0.000 | 0.281±0.000 |
| LMSC | 0.883±0.000 | 0.699±0.000 | 0.746±0.000 | 0.806±0.000 | 0.847±0.003 | 0.739±0.001 | 0.749±0.001 | 0.810±0.001 | 0.442±0.009 | 0.444±0.009 | 0.275±0.007 | 0.318±0.012 |
| MCLES | 0.819±0.000 | 0.637±0.000 | 0.662±0.000 | 0.742±0.000 | 0.921±0.000 | 0.802±0.000 | 0.795±0.000 | 0.945±0.000 | 0.469±0.000 | 0.516±0.000 | 0.337±0.000 | 0.390±0.000 |
| FPMVS-CAG | 0.323±0.000 | 0.030±0.000 | 0.037±0.000 | 0.276±0.000 | 0.406±0.000 | 0.106±0.000 | 0.103±0.000 | 0.304±0.000 | 0.272±0.000 | 0.356±0.000 | 0.182±0.000 | 0.248±0.000 |
| CLR-MVP | 0.626±0.000 | 0.476±0.000 | 0.437±0.000 | 0.597±0.000 | 0.925±0.000 | 0.815±0.000 | 0.851±0.000 | 0.886±0.000 | 0.520±0.000 | 0.533±0.001 | 0.365±0.001 | 0.403±0.001 |
| t-SVD-MSC | 0.858±0.001 | 0.685±0.002 | 0.725±0.002 | 0.789±0.001 | 0.879±0.000 | 0.765±0.000 | 0.784±0.000 | 0.834±0.000 | 0.836±0.005 | 0.852±0.002 | 0.766±0.002 | 0.780±0.002 |
| SM ² SC | 0.934±0.008 | 0.812±0.001 | 0.853±0.003 | 0.887±0.006 | 0.982±0.000 | 0.937±0.000 | 0.952±0.000 | 0.963±0.000 | 0.442±0.008 | 0.453±0.005 | 0.276±0.007 | 0.319±0.007 |
| ETLMSC | 0.872±0.094 | 0.826±0.028 | 0.811±0.082 | 0.855±0.063 | 0.959±0.086 | 0.972±0.058 | 0.949±0.107 | 0.961±0.081 | 0.811±0.066 | 0.874±0.025 | 0.763±0.057 | 0.778±0.054 |
| LMVSC | 0.480±0.000 | 0.242±0.000 | 0.403±0.000 | 0.380±0.000 | 0.517±0.000 | 0.382±0.000 | 0.151±0.000 | 0.394±0.000 | 0.360±0.000 | 0.385±0.000 | 0.198±0.000 | 0.246±0.000 |
| E ² OMVC | 0.849±0.000 | 0.707±0.000 | 0.713±0.000 | 0.783±0.000 | 0.971±0.000 | 0.903±0.000 | 0.920±0.000 | 0.940±0.000 | 0.490±0.000 | 0.477±0.000 | 0.256±0.000 | 0.306±0.000 |
| RMSL | 0.943±0.009 | 0.831±0.005 | 0.862±0.004 | 0.894±0.002 | 0.972±0.002 | 0.905±0.005 | 0.931±0.002 | 0.947±0.004 | 0.511±0.006 | 0.490±0.007 | 0.332±0.010 | 0.372±0.005 |
| CCL-MVC | 0.984±0.000 | 0.951±0.000 | 0.962±0.000 | 0.971±0.000 | 0.996±0.000 | 0.986±0.000 | 0.991±0.000 | 0.993±0.000 | 0.890±0.053 | 0.892±0.019 | 0.832±0.052 | 0.852±0.048 |
| Datasets | UCI-3view | | | | StillDB | | | | MITIndoor | | | |
| Methods | ACC | NMI | AR | F-Score | ACC | NMI | AR | F-Score | ACC | NMI | AR | F-Score |
| AWP | 0.806±0.000 | 0.842±0.000 | 0.759±0.000 | 0.785±0.000 | 0.306±0.000 | 0.093±0.000 | 0.058±0.000 | 0.223±0.000 | 0.499±0.000 | 0.629±0.000 | 0.317±0.000 | 0.329±0.000 |
| MvDSCN | 0.308±0.011 | 0.299±0.013 | 0.158±0.009 | 0.281±0.006 | 0.377±0.023 | 0.245±0.020 | 0.169±0.003 | 0.320±0.015 | 0.084±0.003 | 0.182±0.004 | 0.014±0.002 | 0.037±0.001 |
| OMVFC-LICAG | 0.833±0.000 | 0.811±0.000 | 0.731±0.000 | 0.759±0.000 | 0.376±0.000 | 0.129±0.000 | 0.087±0.000 | 0.273±0.000 | 0.319±0.000 | 0.453±0.000 | 0.157±0.000 | 0.171±0.000 |
| MLAN | 0.874±0.000 | 0.910±0.000 | 0.847±0.000 | 0.864±0.000 | 0.349±0.000 | 0.138±0.000 | 0.098±0.000 | 0.272±0.000 | 0.232±0.010 | 0.408±0.012 | 0.012±0.009 | 0.041±0.003 |
| GMC | 0.736±0.000 | 0.815±0.000 | 0.678±0.000 | 0.713±0.000 | 0.251±0.000 | 0.078±0.000 | 0.005±0.000 | 0.278±0.000 | 0.099±0.000 | 0.204±0.000 | 0.003±0.000 | 0.032±0.000 |
| UOMvSC | 0.981±0.000 | 0.956±0.000 | 0.958±0.000 | 0.962±0.000 | 0.328±0.000 | 0.131±0.000 | 0.084±0.000 | 0.246±0.000 | 0.344±0.000 | 0.506±0.000 | 0.064±0.000 | 0.088±0.000 |
| EOMSC-CA | 0.545±0.000 | 0.673±0.000 | 0.459±0.000 | 0.533±0.000 | 0.308±0.000 | 0.127±0.000 | 0.085±0.000 | 0.245±0.000 | 0.147±0.000 | 0.298±0.000 | 0.042±0.000 | 0.066±0.000 |
| LMSC | 0.893±0.000 | 0.815±0.000 | 0.783±0.000 | 0.805±0.000 | 0.327±0.003 | 0.136±0.003 | 0.084±0.011 | 0.269±0.005 | 0.384±0.006 | 0.506±0.005 | 0.243±0.005 | 0.254±0.004 |
| MCLES | 0.941±0.004 | 0.891±0.008 | 0.877±0.009 | 0.889±0.008 | 0.338±0.000 | 0.153±0.000 | 0.098±0.000 | 0.264±0.000 | — | — | — | — |
| FPMVS-CAG | 0.722±0.000 | 0.744±0.000 | 0.645±0.000 | 0.683±0.000 | 0.328±0.000 | 0.124±0.000 | 0.089±0.000 | 0.251±0.000 | 0.204±0.000 | 0.390±0.000 | 0.085±0.000 | 0.108±0.000 |
| CLR-MVP | 0.965±0.000 | 0.920±0.001 | 0.924±0.001 | 0.932±0.001 | 0.337±0.002 | 0.127±0.003 | 0.095±0.001 | 0.273±0.002 | — | — | — | — |
| t-SVD-MSC | 0.830±0.000 | 0.884±0.005 | 0.786±0.003 | 0.800±0.004 | 0.347±0.010 | 0.130±0.004 | 0.088±0.003 | 0.255±0.004 | 0.684±0.005 | 0.750±0.007 | 0.555±0.005 | 0.562±0.008 |
| SM ² SC | 0.961±0.001 | 0.914±0.001 | 0.914±0.001 | 0.923±0.001 | 0.452±0.002 | 0.336±0.002 | 0.312±0.002 | 0.370±0.002 | 0.477±0.009 | 0.583±0.006 | 0.321±0.006 | 0.332±0.006 |
| ETLMSC | 0.958±0.078 | 0.977±0.028 | 0.953±0.069 | 0.958±0.062 | 0.604±0.043 | 0.520±0.015 | 0.423±0.029 | 0.523±0.024 | 0.775±0.040 | 0.899±0.011 | 0.729±0.037 | 0.733±0.036 |
| LMVSC | 0.790±0.000 | 0.756±0.000 | 0.643±0.000 | 0.681±0.000 | 0.317±0.000 | 0.189±0.000 | 0.066±0.000 | 0.239±0.000 | 0.371±0.000 | 0.522±0.000 | 0.112±0.000 | 0.132±0.000 |
| E ² OMVC | 0.974±0.000 | 0.941±0.000 | 0.943±0.000 | 0.949±0.000 | 0.321±0.000 | 0.130±0.000 | 0.089±0.000 | 0.265±0.000 | 0.404±0.000 | 0.550±0.000 | 0.173±0.000 | 0.191±0.000 |
| RMSL | 0.578±0.013 | 0.511±0.014 | 0.407±0.017 | 0.474±0.007 | 0.356±0.003 | 0.131±0.001 | 0.090±0.002 | 0.243±0.001 | 0.279±0.004 | 0.372±0.003 | 0.125±0.005 | 0.139±0.002 |
| CCL-MVC | 0.988±0.037 | 0.996±0.013 | 0.988±0.037 | 0.990±0.033 | 0.752±0.077 | 0.682±0.042 | 0.597±0.079 | 0.666±0.066 | 0.860±0.038 | 0.946±0.011 | 0.842±0.038 | 0.844±0.037 |

ABLATION STUDY & CONVERGENCE

Significance of cross-view diversity

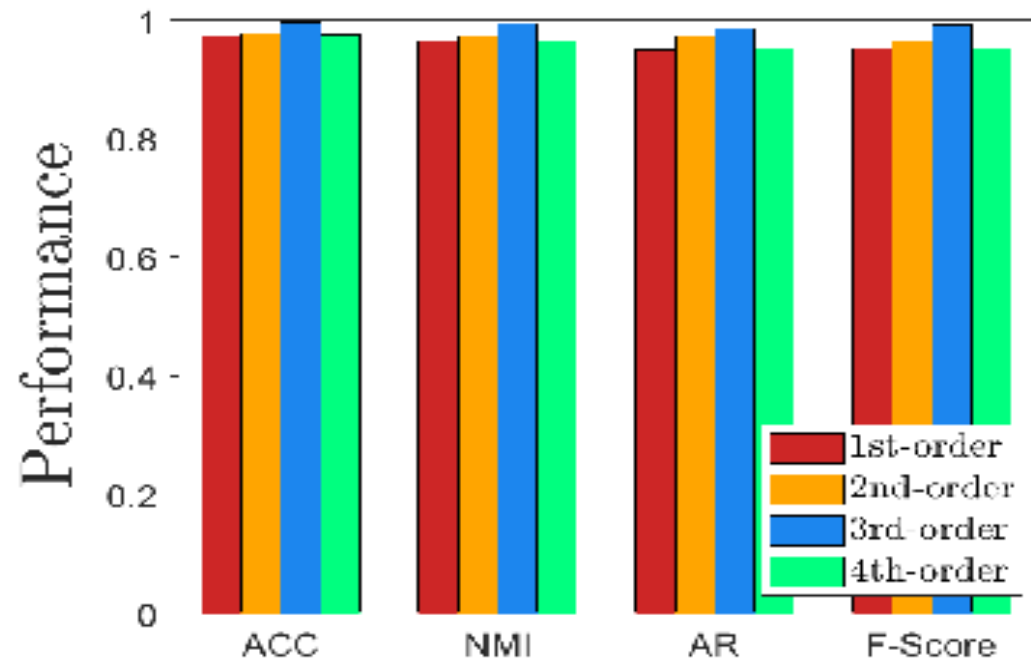


(a) BBC-Sport

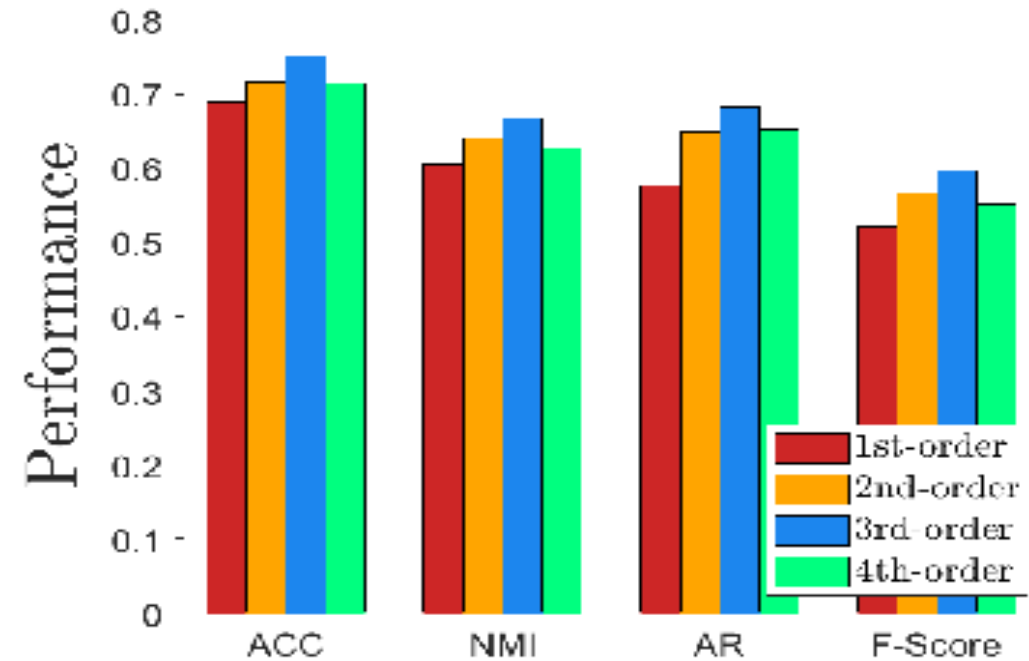


(b) StillDB

CROSS-ORDER NEIGHBOR INFORMATION

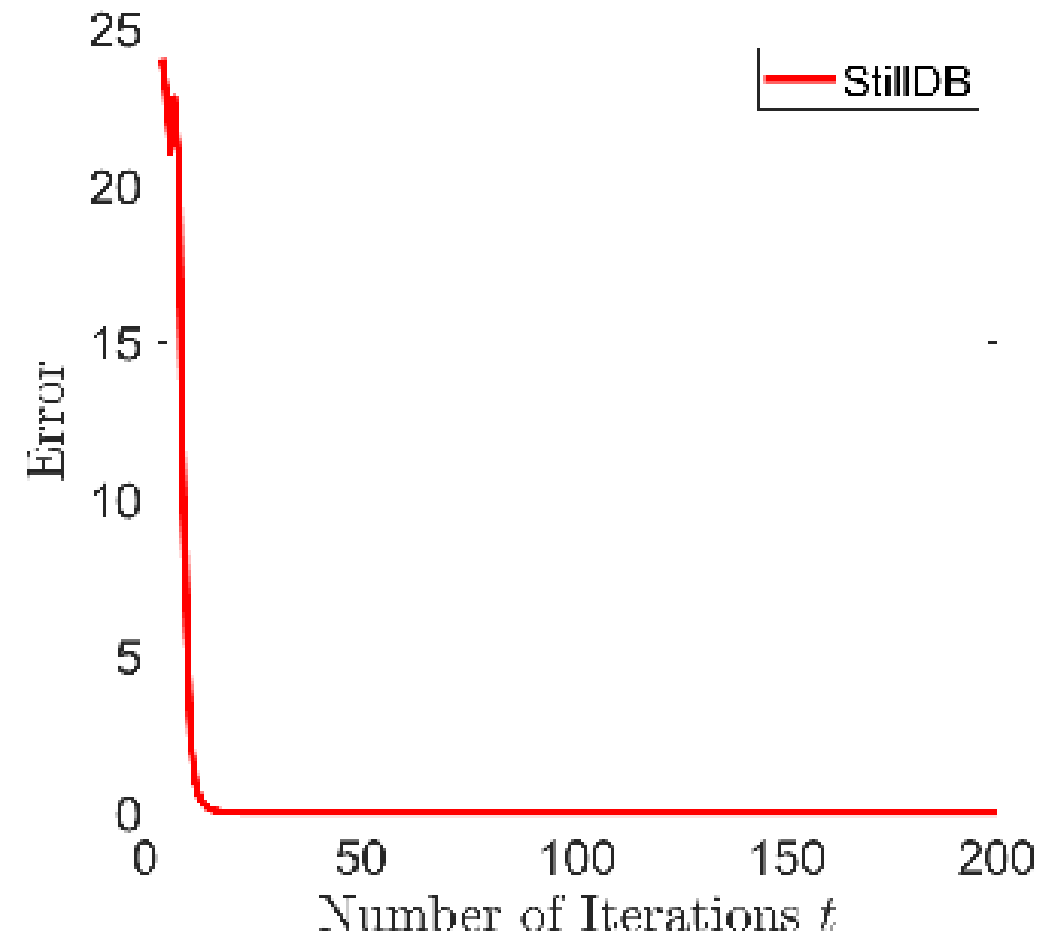
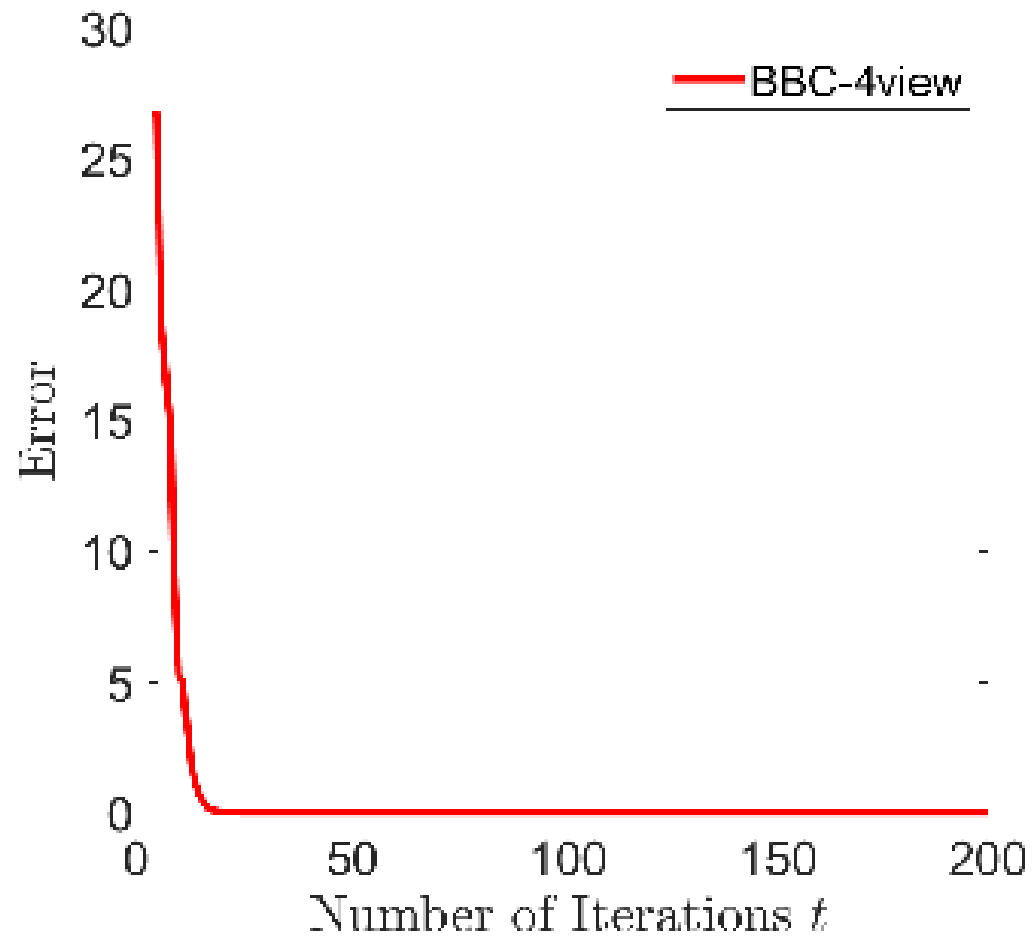


(a) BBC-Sport



(b) StillDB

CONVERGENCE CURVES ON SAMPLE DATASETS



BRIEF CONCLUSION OF TOPIC 3

- CCL-MVC for enhanced MVC with diversity and cross-order info
- Efficient optimization with convergence guarantee
- Superior performance experimentally validated

Future Work:

- More accurate approximation of tensor rank

TOPIC 4 – NEW DEEP LEARNING MODEL FOR TIME SERIES CLASSIFICATION

Motivation

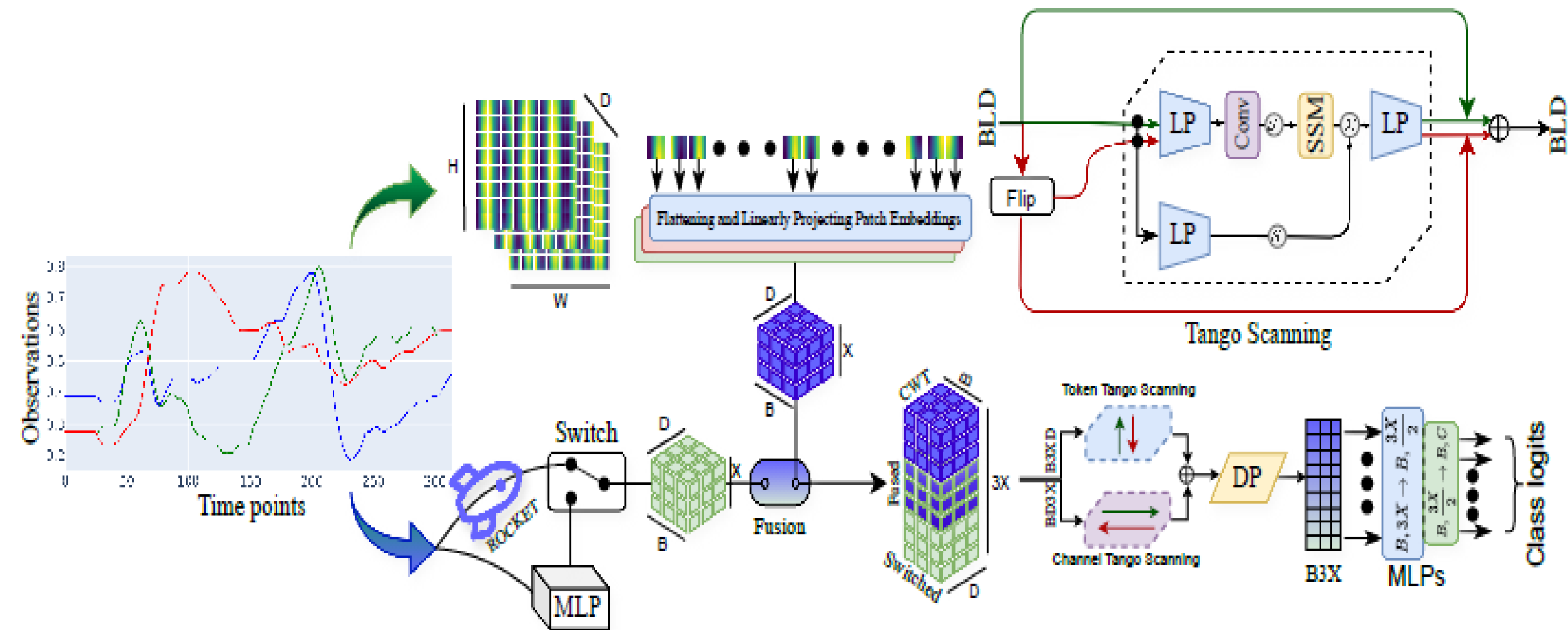
- Importance of time series classification (TSC)
 - Structured format; mixed types; predominant in various domains
- Challenges with existing deep learning models for TSC
 - Classical methods (DTW, XGBoost): accuracy, long-range dependency
 - Deep learning models (Rocket, LSTM, TCN): accuracy, LRD
 - Transformer-based models (Informer, AutoFormer, FlowFormer, FedFormer): efficiency, scalability
- Need for an efficient, accurate, scalable approach
 - Also, existing models do not consider inversion invariance

NEW MODEL: TSCMAMBA

Key Innovations

- Captures features that are robust to time shifting and time inversion
- Use multi-view framework to integrate time-frequency features at global and local scales for classification
- First to leverage SSM modules (Mamba) for TSC with linear scalability and small memory footprints
- Creates a new Mamba scanning scheme (Tango scanning): capturing inversion-invariant features

MODEL ARCHITECTURE



DATASETS FOR EVALUATIONS

| | Datasets | Channels | Length | Train | Test | Classes | Domain |
|---------------------|-----------------------------|----------|--------|-------|------|---------|----------------------------|
| Benchmark datasets | EthanolConcentration (EC) | 3 | 1751 | 261 | 263 | 4 | Alcohol Industry |
| | FaceDetection (FD) | 144 | 62 | 5890 | 3524 | 2 | Face (250Hz) |
| | Handwriting (HW) | 3 | 152 | 150 | 850 | 26 | Smart Watch |
| | Heartbeat (HB) | 61 | 405 | 204 | 205 | 2 | Clinical |
| | JapaneseVowels (JV) | 12 | 29 | 270 | 370 | 9 | Audio |
| | PEMS-SF (PS) | 963 | 144 | 267 | 173 | 7 | Transportation |
| | SelfRegulationSCP1 (SCP1) | 6 | 896 | 268 | 293 | 2 | Health (256Hz) |
| | SelfRegulationSCP2 (SCP2) | 7 | 1152 | 200 | 180 | 2 | Health (256Hz) |
| | SpokenArabicDigits (SA) | 13 | 93 | 6599 | 2199 | 10 | Voice (11025Hz) |
| | UWaveGestureLibrary (UG) | 3 | 315 | 120 | 320 | 8 | Gesture |
| Additional datasets | AtrialFibrillation (AF) | 2 | 640 | 15 | 15 | 3 | ECG |
| | BasicMotions (BM) | 6 | 100 | 40 | 40 | 4 | Human Activity Recognition |
| | Cricket (CR) | 6 | 1197 | 108 | 72 | 12 | Human Activity Recognition |
| | FingerMovements (FM) | 28 | 50 | 316 | 100 | 2 | EEG |
| | HandMovementDirection (HMD) | 10 | 400 | 160 | 74 | 4 | EEG |
| | MotorImagery (MI) | 64 | 3000 | 278 | 100 | 2 | EEG |
| | PenDigits (PD) | 2 | 8 | 7494 | 3498 | 10 | Motion |
| | PhonemeSpectra (PHS) | 11 | 217 | 3315 | 3353 | 39 | Audio |
| | RacketSports (RS) | 6 | 30 | 151 | 152 | 4 | Human Activity Recognition |
| | StandWalkJump (SWJ) | 4 | 2500 | 12 | 15 | 3 | ECG |

EXPERIMENTAL RESULTS (20 BASELINES)

Classification Accuracy (%). The . symbol in Transformer models denotes *former used.
The best average result and rank: in **bold**; the second best: underlined.
The ranks: Wilcoxon signed-rank test (lower is better).

| Datasets | Methods | | | | | | | | | | | | | | | | | | | | |
|----------|---------------|-------------------|------------------|----------------|------------------|----------------|---------------|-----------------|---------------|---------------|----------------|-----------------|--------------------|----------------|----------------|-----------------|-------------------|---------------------|--------------------|-------------------|------------------|
| | DTW (1994) | XGBoost (2016) | Rocket (2020) | LSTM (1997) | LSTNet (2018) | LSSL (2022) | TCN (2019) | Trans (2017) | Re. (2020) | In. (2021) | Pyra (2021) | Auto. (2021) | Station. (2022) | FED. (2022) | ETS. (2022) | Flow. (2022) | DLinear (2023) | LightTS. (2022a) | TimesNet (2023) | TSLANet (2024) | TSCMamba Ours |
| EC | 32.3 | 43.7 | 45.2 | 32.3 | 39.9 | 31.1 | 28.9 | 32.7 | 31.9 | 31.6 | 30.8 | 31.6 | 32.7 | 31.2 | 28.1 | 33.8 | 32.6 | 29.7 | 35.7 | 30.4 | 62.0 |
| FD | 52.9 | 63.3 | 64.7 | 57.7 | 65.7 | 66.7 | 52.8 | 67.3 | 68.6 | 67.0 | 65.7 | 68.4 | 68.0 | 66.0 | 66.3 | 67.6 | 68.0 | 67.5 | 68.6 | 66.8 | 69.4 |
| HW | 28.6 | 15.8 | 58.8 | 15.2 | 25.8 | 24.6 | 53.3 | 32.0 | 27.4 | 32.8 | 29.4 | 36.7 | 31.6 | 28.0 | 32.5 | 33.8 | 27.0 | 26.1 | 32.1 | 57.9 | 53.3 |
| HB | 71.7 | 73.2 | 75.6 | 72.2 | 77.1 | 72.7 | 75.6 | 76.1 | 77.1 | 80.5 | 75.6 | 74.6 | 73.7 | 73.7 | 71.2 | 77.6 | 75.1 | 75.1 | 78.0 | 77.6 | 76.6 |
| JV | 94.9 | 86.5 | 96.2 | 79.7 | 98.1 | 98.4 | 98.9 | 98.7 | 97.8 | 98.9 | 98.4 | 96.2 | 99.2 | 98.4 | 95.9 | 98.9 | 96.2 | 96.2 | 98.4 | 99.2 | 97.0 |
| PS | 71.1 | 98.3 | 75.1 | 39.9 | 86.7 | 86.1 | 68.8 | 82.1 | 82.7 | 81.5 | 83.2 | 82.7 | 87.3 | 80.9 | 86.0 | 83.8 | 75.1 | 88.4 | 89.6 | 83.8 | 90.2 |
| SCP1 | 77.7 | 84.6 | 90.8 | 68.9 | 84.0 | 90.8 | 84.6 | 92.2 | 90.4 | 90.1 | 88.1 | 84.0 | 89.4 | 88.7 | 89.6 | 92.5 | 87.3 | 89.8 | 91.8 | 91.8 | 92.5 |
| SCP2 | 53.9 | 48.9 | 53.3 | 46.6 | 52.8 | 52.2 | 55.6 | 53.9 | 56.7 | 53.3 | 53.3 | 50.6 | 57.2 | 54.4 | 55.0 | 56.1 | 50.5 | 51.1 | 57.2 | 61.7 | 66.7 |
| SA | 96.3 | 69.6 | 71.2 | 31.9 | 100.0 | 100.0 | 95.6 | 98.4 | 97.0 | 100.0 | 99.6 | 100.0 | 100.0 | 100.0 | 100.0 | 98.8 | 81.4 | 100.0 | 99.0 | 99.9 | 99.0 |
| UG | 90.3 | 75.9 | 94.4 | 41.2 | 87.8 | 85.9 | 88.4 | 85.6 | 85.6 | 85.6 | 83.4 | 85.9 | 87.5 | 85.3 | 85.0 | 86.6 | 82.1 | 80.3 | 85.3 | 91.3 | 93.8 |
| Avg. | 67.0 | 66.0 | 72.5 | 48.6 | 71.8 | 70.9 | 70.3 | 71.9 | 71.5 | 72.1 | 70.8 | 71.1 | 72.7 | 70.7 | 71.0 | 73.0 | 67.5 | 70.4 | 73.6 | 76.04 | 80.05 |
| Rank | 15.20 | 15.55 | 10.25 | 19.55 | 10.40 | 11.70 | 12.40 | 9.40 | 9.95 | 8.90 | 12.80 | 11.50 | 7.30 | 12.40 | 12.85 | 6.45 | 14.60 | 12.65 | 6.40 | 6.40 | 4.35 |

COMPUTATIONAL EFFICIENCY

FLOPs comparison among the top performing methods.

The values: in GigaFLOPS (G) or TeraFlops (T), 1 TFLOPs=1000 GFLOPs

A lower value: better computational efficiency

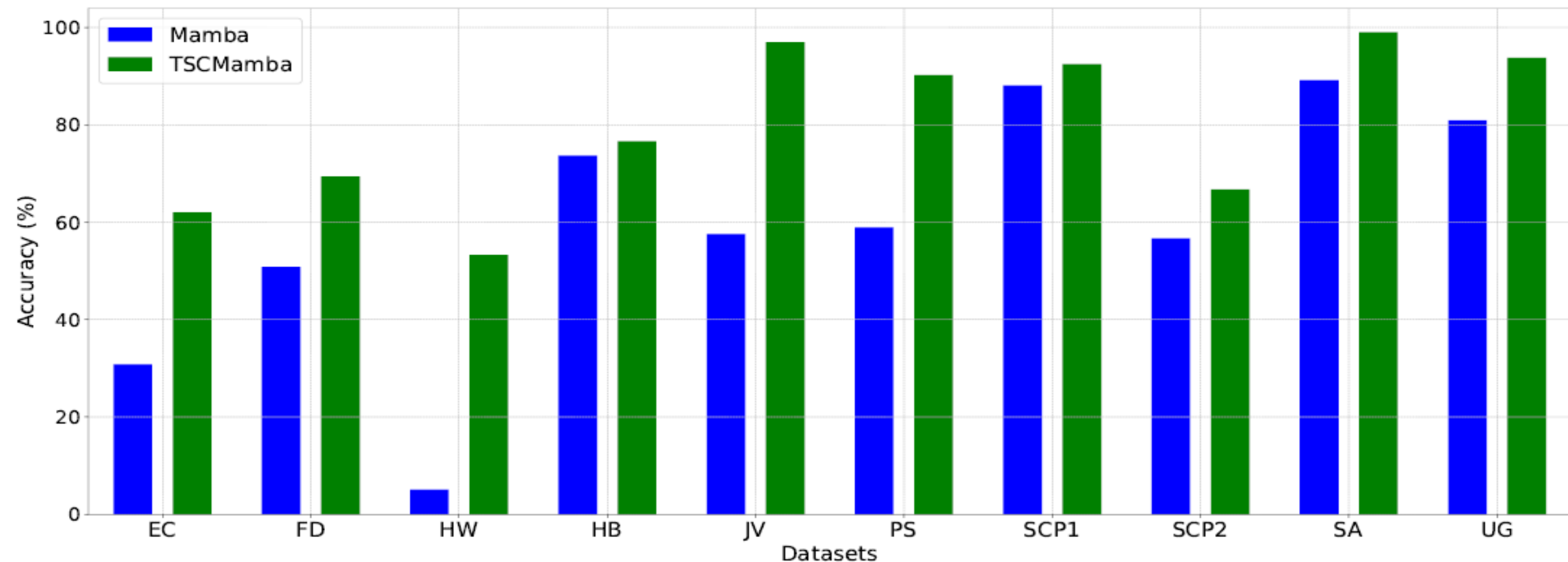
| Methods | EC | FD | HW | HB | JV | PS | SCP1 | SCP2 | SA | UG |
|----------------------------|-------|---------|---------|---------|--------|---------------|---------|---------|--------------|---------|
| Flow. Wu et al. (2022) | 1.06T | 37.97G | 92.21G | 246.37G | 15.76G | 94.02G | 542.64G | 697.74G | 50.33G | 190.82G |
| TimesNet. Wu et al. (2023) | 1.11T | 161.93G | 115.88G | 182.69G | 48.15G | 74.18G | 503.62G | 2.33T | 26.00G | 247.73G |
| TSCMamba (Ours) | 1.69G | 11.53G | 27.24G | 8.39G | 12.33G | 2.84T | 3.42G | 11.11G | 0.78G | 13.86G |

ADDITIONAL EXPERIMENTAL RESULTS

Additional classification results on the UEA datasets in accuracy (as %).
The ranks: Wilcoxon signed-rank test (lower is better).

| Dataset | TSCMamba Ours | TSLANet (2024) | GPT4TS (2023) | TimesNet (2023) | ROCKET (2020) | CrossF. (2023) | PatchTST (2023) | MLP (2023) | TS-TCC (2021) | TS2VEC (2022) |
|-----------------------|------------------|-------------------|------------------|--------------------|------------------|-------------------|--------------------|--------------------|------------------|------------------|
| AtrialFibrillation | 67.00 | 40.00 | 33.33 | 33.33 | 20.00 | 46.66 | <u>53.33</u> | 46.66 | 33.33 | <u>53.33</u> |
| BasicMotions | 100.00 | <u>100.00</u> | 92.50 | <u>100.00</u> | 100.00 | 90.00 | 92.50 | 85.00 | 100.00 | 92.50 |
| Cricket | 98.61 | <u>98.61</u> | 8.33 | 87.50 | <u>98.61</u> | 84.72 | 84.72 | 91.67 | 93.06 | 65.28 |
| FingerMovements | 69.00 | 61.00 | 57.00 | 59.38 | 61.00 | <u>64.00</u> | 62.00 | <u>64.00</u> | 44.00 | 51.00 |
| HandMovementDirection | 71.62 | 52.70 | 18.92 | 50.00 | 50.00 | 58.11 | 58.11 | 58.11 | <u>64.86</u> | 32.43 |
| MotorImagery | 62.00 | <u>62.00</u> | 50.00 | 51.04 | 53.00 | 61.00 | 61.00 | 61.00 | 47.00 | 47.00 |
| PenDigits | 98.54 | <u>98.94</u> | 97.74 | 98.19 | 97.34 | 93.65 | 99.23 | 92.94 | 98.51 | 97.40 |
| PhonemeSpectra | <u>24.66</u> | 17.75 | 3.01 | 18.24 | 17.60 | 7.55 | 11.69 | 7.10 | 25.92 | 8.23 |
| RacketSports | 91.45 | <u>90.79</u> | 76.97 | 82.64 | 86.18 | 81.58 | 84.21 | 78.95 | 84.87 | 74.34 |
| StandWalkJump | 73.33 | 46.67 | 33.33 | 53.33 | 46.67 | 53.33 | <u>60.00</u> | <u>60.00</u> | 40.00 | 46.67 |
| Average | 75.62 | <u>66.85</u> | 47.11 | 63.36 | 63.04 | 64.06 | 66.68 | 64.54 | 63.15 | 56.82 |
| Rank | 1.65 | <u>3.90</u> | 8.60 | 5.70 | 5.70 | 6.00 | 4.35 | 5.95 ₄₆ | 5.45 | 7.70 |

COMPARISON WITH MAMBA



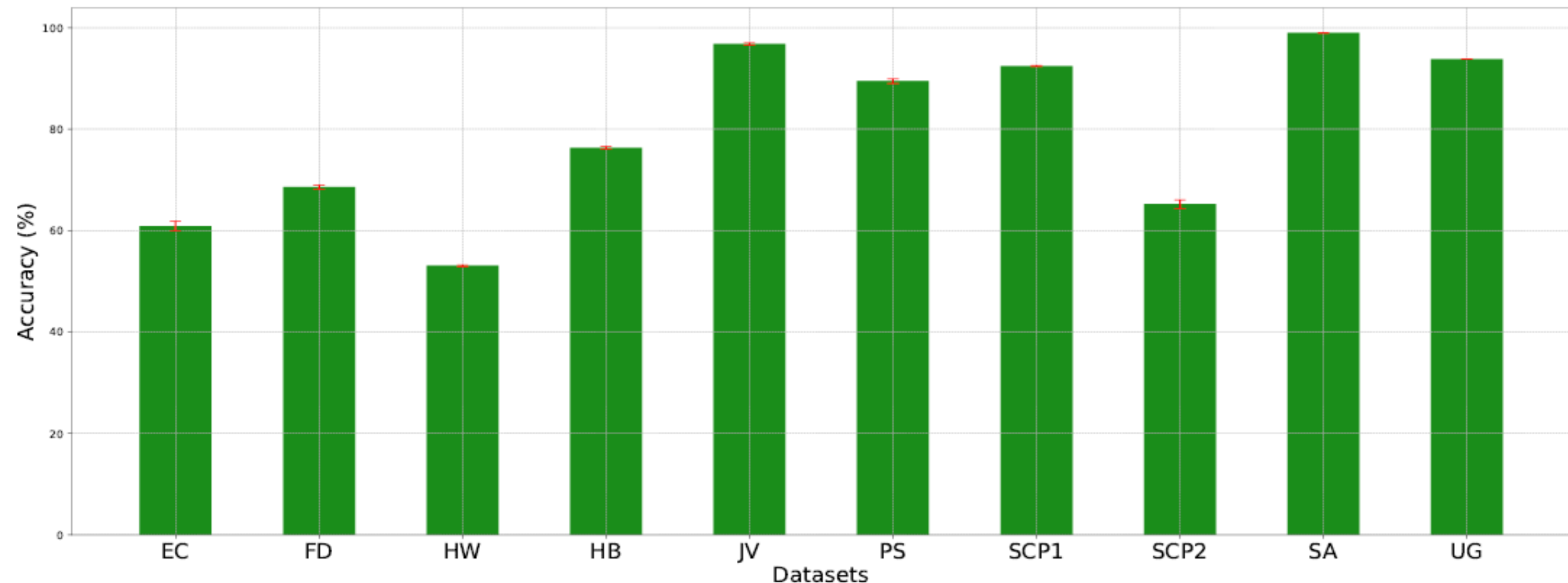
TSCMamba (using proposed Tango scanning) in comparison with directly applying regular Mamba module.

ABLATION STUDY (COMPONENT-WISE)

Ablation experiments on particular components in our method.

| Mamba | Avg.Pool | ROCKET | AF | EC | FD | HW | HB | JV | PS | SCP1 | SCP2 | SA | UG | Avg. |
|-------|----------|--------|----|------|------|------|------|------|------|------|------|------|------|-------|
| ✓ | ✓ | ✓ | ✓ | 62.0 | 57.0 | 53.3 | 74.1 | 93.0 | 90.2 | 92.5 | 66.7 | 94.1 | 93.8 | 77.67 |
| ✗ | ✓ | ✓ | ✓ | 33.1 | 63.2 | 34.1 | 73.2 | 85.4 | 81.5 | 86.7 | 57.2 | 74.0 | 89.1 | 67.75 |
| ✓ | ✗ | ✓ | ✓ | 31.6 | 64.2 | 52.0 | 74.1 | 94.1 | 63.0 | 86.7 | 60.6 | 96.7 | 92.8 | 71.58 |
| ✓ | ✓ | ✗ | ✓ | 31.6 | 69.4 | 24.8 | 76.6 | 97.0 | 87.3 | 91.8 | 58.3 | 97.6 | 86.2 | 72.06 |
| ✓ | ✓ | ✓ | ✗ | 30.0 | 51.5 | 49.3 | 72.7 | 91.4 | 84.4 | 88.7 | 58.9 | 90.0 | 90.3 | 70.72 |

MEAN AND STD DEV OVER DIFFERENT RUNS



Performance of TSCMamba over 5 random runs.
Mean performance: green bars,
Standard deviation: red error bars (very small).

BRIEF SUMMARY OF TIME SERIES CLASSIFICATION

- We create a new model for time series classification, TSCMamba
- It leverages a new scanning scheme for Mamba to take advantage of inversion invariance
- It shows better performance than SOTA models (> 10 models) on 20 benchmark time series datasets (in both averaged acc. and rank)
- It is efficient - typically uses a small fraction of FLOPS than other top performing models

REFERENCES

1. MA Ahamed, Q Cheng (2024). MambaTab: A plug-and-play model for learning tabular data. IEEE MIPR. Code available at GitHub.
2. MA Ahamed, Q Cheng (2024). TimeMachine: A Time Series is Worth 4 Mambas for Long-term Forecasting. ECAI. Code Available at GitHub.
3. C Peng, Y Liu, K Kang, Y Chen, X Wu, A Cheng, Z Kang, C Chen, and Q Cheng (2022). Hyperspectral image denoising using nonconvex local low-rank and sparse separation with spatial-spectral total variation regularization. IEEE Transactions on Geoscience and Remote Sensing, 60:1–17.
4. C Peng, Z Kang, H Li, and Q Cheng (2015). Subspace clustering using log-determinant rank approximation. ACM KDD, pp. 925–934.
5. Z Kang, C Peng, Q Cheng (2017). Twin learning for similarity and clustering: A unified kernel approach. AAAI.
6. Z Kang, C Peng, Q Cheng (2017). Kernel-driven similarity learning. Neurocomputing. 210-219.

REFERENCES

7. C Peng, K Zhang, Y Chen, C Chen, Q Cheng (2024). Cross-View Diversity Embedded Consensus Learning for Multi-View Clustering. IJCAI.
8. MA Atik, Q Cheng (2024). TSCMamba: Mamba Meets Multi-View Learning for Time Series Classification. arXiv preprint arXiv:2406.04419



Thank you.